

Basics of rubidium-xenon spin-exchange optical pumping

Magnetising xenon gas

Graham Norquay

Aarhus MR workshop 2024

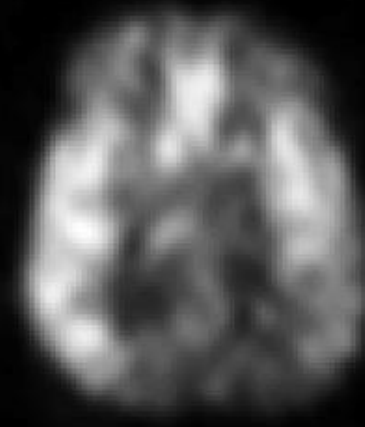
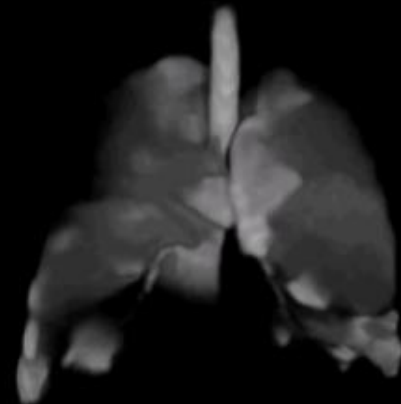
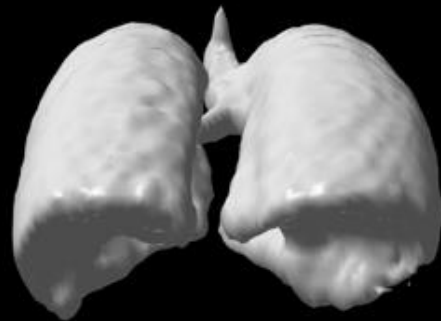
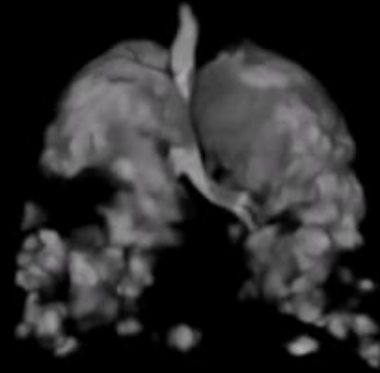
g.norquay@sheffield.ac.uk

Hyperpolarised ^{129}Xe MRI

Healthy



COPD



Human brain

Rao et al,
Radiology, 286,
2018



Human kidneys

Chacon-Caldera
et al., MRM(83)
2019

Gas-phase ^{129}Xe

Dissolved-phase ^{129}Xe

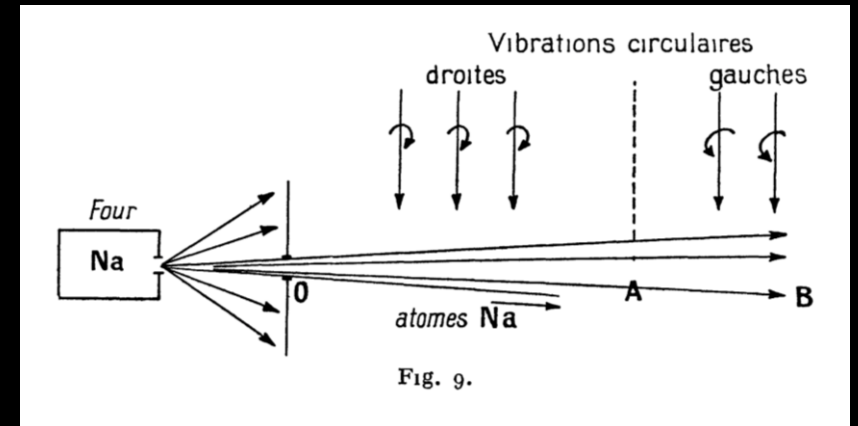
Optical pumping



Alfred Kastler

Awarded 1966 Nobel prize in physics for his work

A. Kastler. "Some suggestions concerning the production and detection by optical means of inequalities in the populations of levels of spatial quantization in atoms. Application to the Stern and Gerlach and magnetic resonance experiments. *J. Phys. Radium*, **11**, 255. (1950)



“The use of circularly polarised light creates an asymmetry of population between negative m levels and positive m levels, the direction of this asymmetry being able to be reversed by reversing the direction of circular polarisation of the incident light”

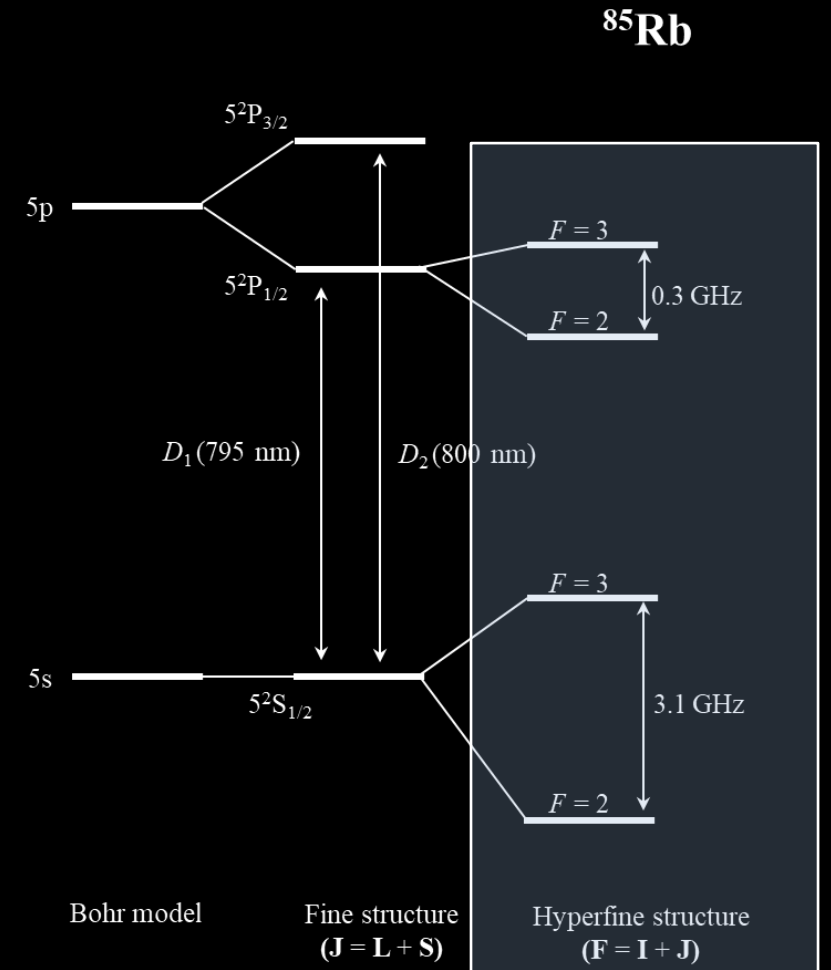
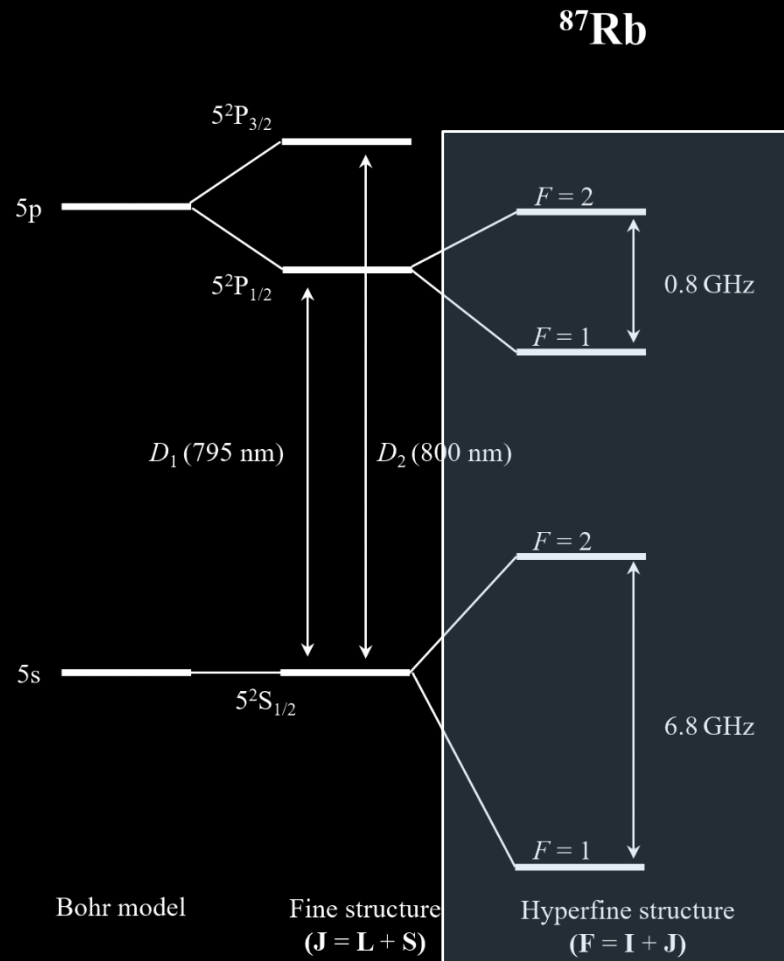
Optical pumping with alkali metals

- λ in visible and near-IR (590-865 nm) – compatible with inexpensive and powerful laser sources
- High volatility – highly dense vapours at relatively low temperatures [MP = 27°C (Fr) to 181°C (Li)]
- Single valence electron in *s* subshell – facilitates comparison between theory and experiment

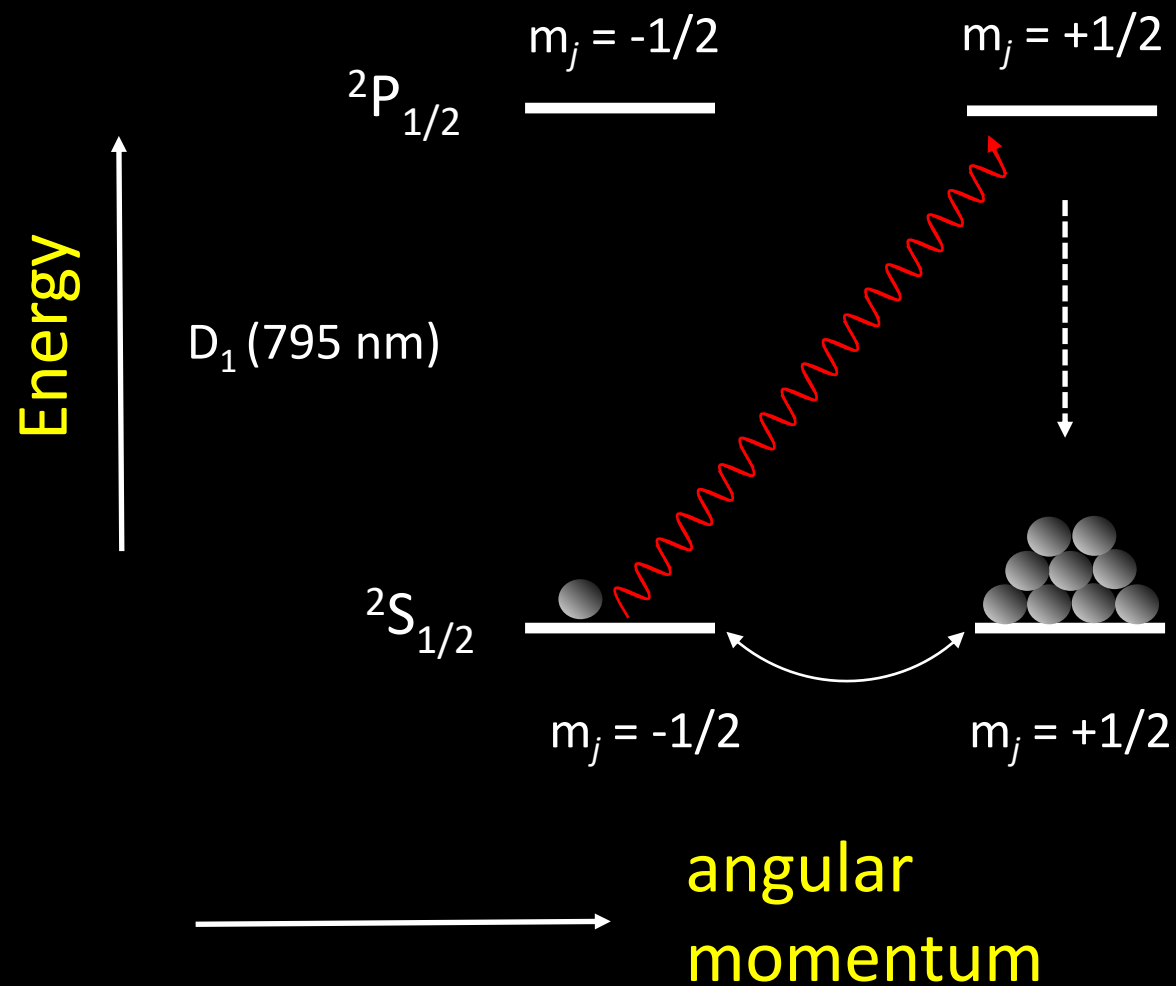
	Li	Na	K	Rb	Cs	Fr
Z	3	11	19	37	55	87
Configuration	[He]2s	[Ne]3s	[Ar]4s	[Kr]5s	[Xe]6s	[Rn]7s
IP (eV)	5.3917	5.1391	4.3407	4.1771	3.8939	4.073
$\lambda(S-P_{1/2})$ (Å)	6709.77	5897.56	7701.08	7949.78	8945.93	8171.66
$\lambda(S-P_{3/2})$ (Å)	6709.62	5891.58	7667.01	7802.41	8523.47	7181.85
ΔE_{FS} (cm ⁻¹)	0.34	17.20	57.71	237.60	554.04	1687
$\tau(nP_{1/2})$ (ns)	27.10 [8]	16.28 [9]	26.69 [10]	27.75 [11]	34.88 [12]	29.45 [13]
$f_{1/2}$	0.249	0.320	0.333	0.341	0.344	0.339
$\tau(nP_{3/2})$ (ns)	27.10 [8]	16.23 [9]	26.34 [10]	26.25 [11]	30.462 [12]	21.0 [14]
$f_{3/2}$	0.497	0.641	0.669	0.695	0.715	0.734
μ_{ns}	0.399 – 0.061 <i>E</i>	1.348 – 0.132 <i>E</i>	2.180 – 0.314 <i>E</i>	3.130 – 0.419 <i>E</i>	4.048 – 0.573 <i>E</i>	5.07 – 0.556 <i>E</i>
μ_{np}	0.047 + 0.050 <i>E</i>	0.854 – 0.258 <i>E</i>	1.711 – 0.542 <i>E</i>	2.645 – 0.681 <i>E</i>	3.568 – 0.889 <i>E</i>	
μ_{nd}	0.002 + 0.009 <i>E</i>	0.015 + 0.081 <i>E</i>	0.278 + 2.137 <i>E</i>	1.353 + 1.760 <i>E</i>	2.476 + 0.372 <i>E</i>	3.41 – 0.095 <i>E</i>

Energy states of rubidium

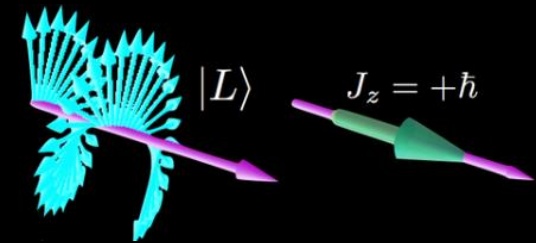
- Abundance: ^{87}Rb (27.8%), ^{85}Rb (82.2%)
- Nuclear spin: $I_{87} = 3/2$, $I_{85} = 5/2$



Optical pumping with rubidium



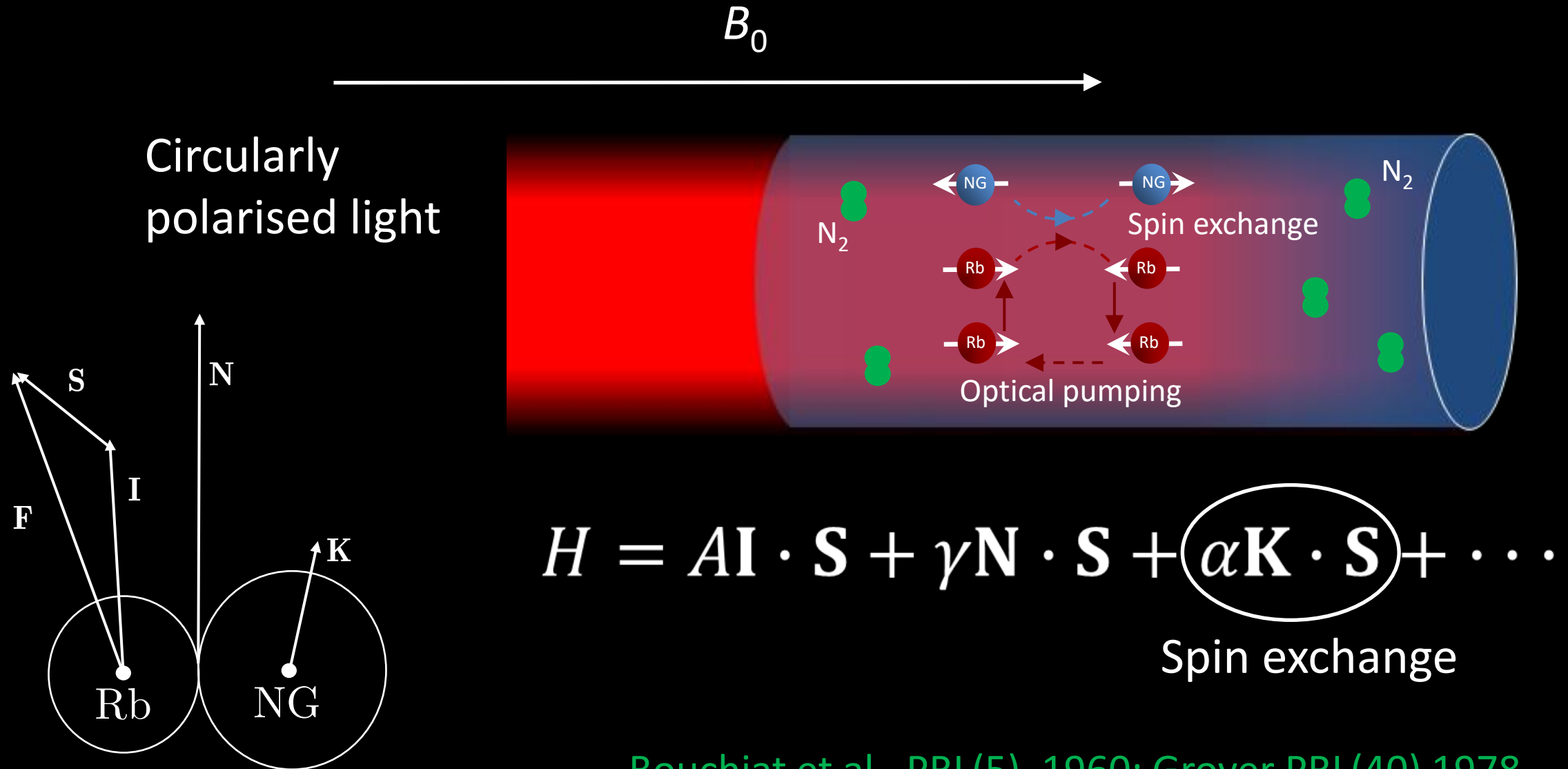
Left-circularly polarised light parallel to B_z



Selection rule:

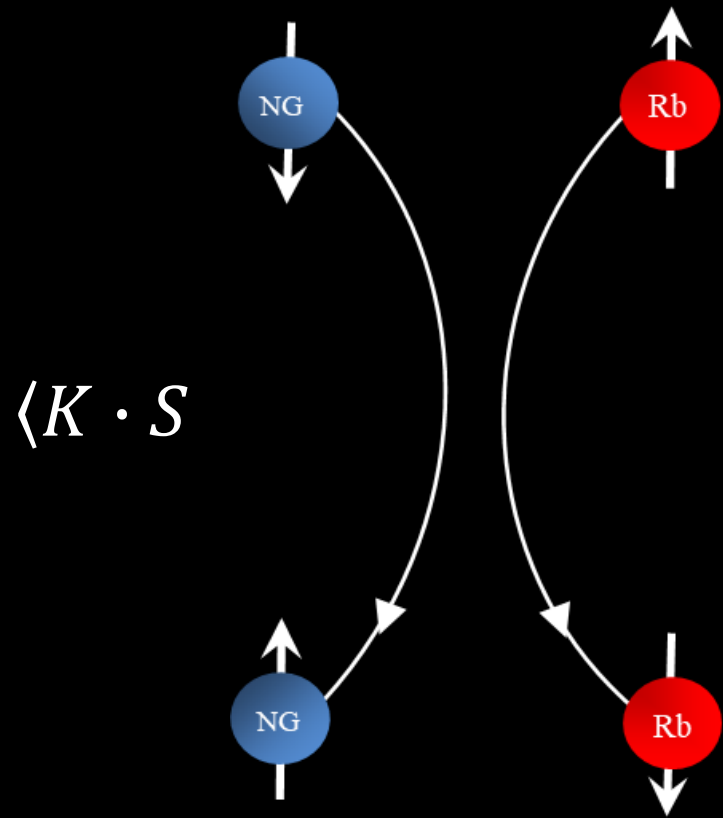
$$\Delta m_j = +1$$

Mixing polarised rubidium vapour with noble gases: SEOP



Bouchiat et al., PRL(5), 1960; Grover PRL(40) 1978

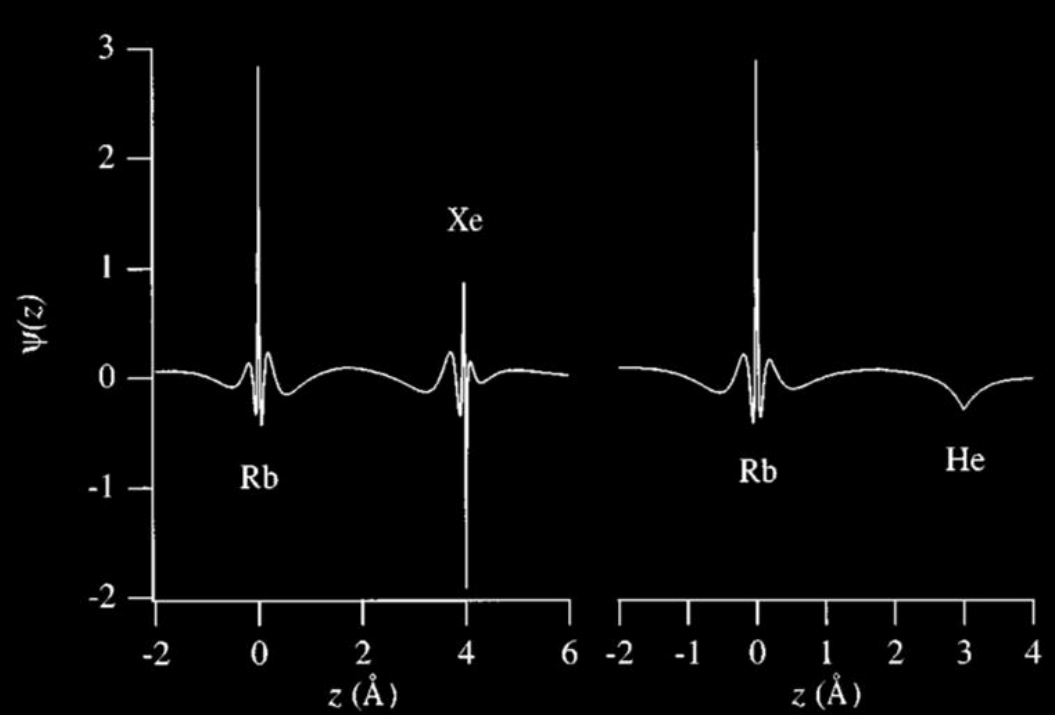
Spin-exchange optical pumping with noble gases



Binary spin-exchange rate:

$$\gamma_{se} = [\text{Rb}] \gamma' \approx 10^{14} \times \begin{cases} 6.8 \times 10^{-20} \text{ cm}^3/\text{s} & \text{He} \\ 2.2 \times 10^{-16} \text{ cm}^3/\text{s} & \text{Xe} \end{cases}$$

$$\approx \begin{cases} (40 \text{ hr})^{-1} & \text{He} \\ (50 \text{ sec})^{-1} & \text{Xe} \end{cases}$$



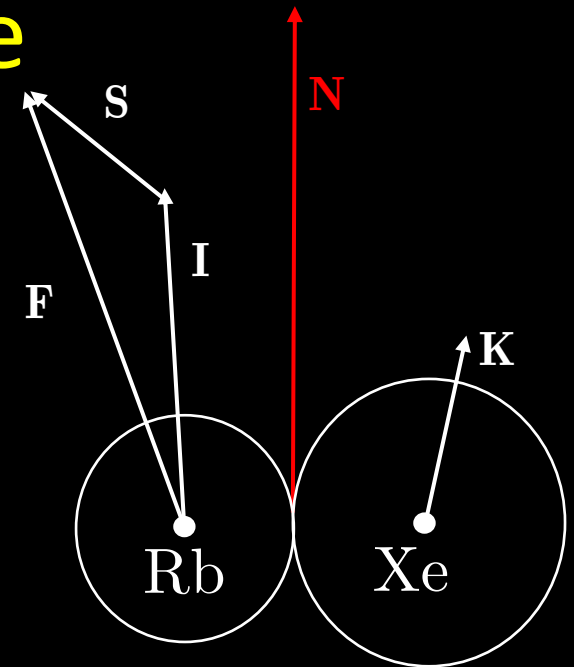
Walker&Happer RMP(69), 1997

^{129}Xe readily destroys Rb electronic polarisation

$$\Gamma_{\text{Rb}}(1 \text{ amagat}) = \begin{cases} 2.4 \times 10^5 / \text{s} & \text{Xe} \\ 45 / \text{s} & \text{He} \end{cases}$$

$$H = A\mathbf{I} \cdot \mathbf{S} + \gamma\mathbf{N} \cdot \mathbf{S} + \alpha\mathbf{K} \cdot \mathbf{S} + \dots$$

Spin-rotation interaction at xenon core



Challenge: need to use lean mixtures of Xe or low Rb vapour densities

Two methods to polarise ^{129}Xe with spin-exchange optical pumping

Continuous-flow: ^{129}Xe polarised with cryogenic Xe accumulation



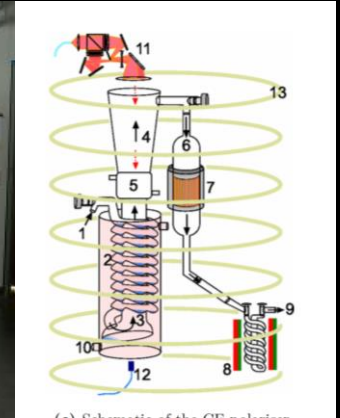
Norquay et al., PRL(121), 2018



Polarean 9820



Xemed, XeBox-E10, Ruset et al., PRL(96), 2006

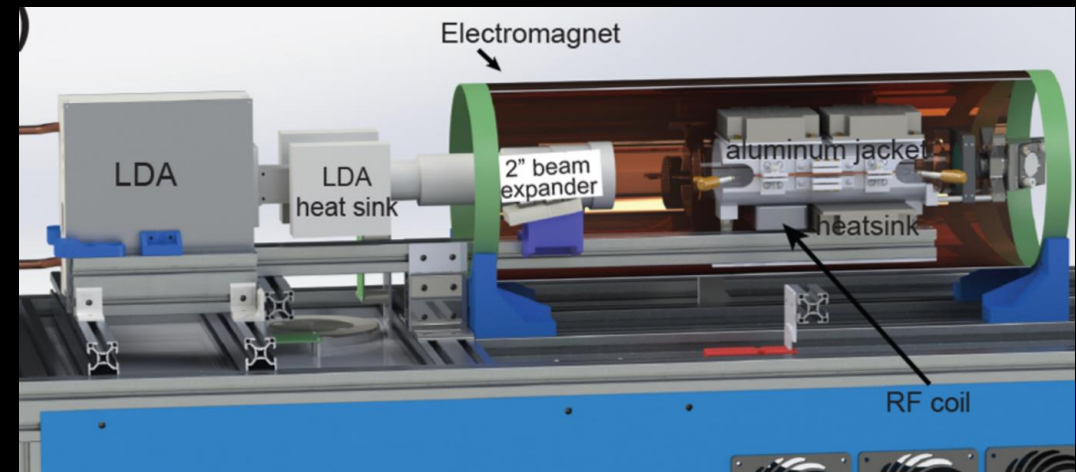
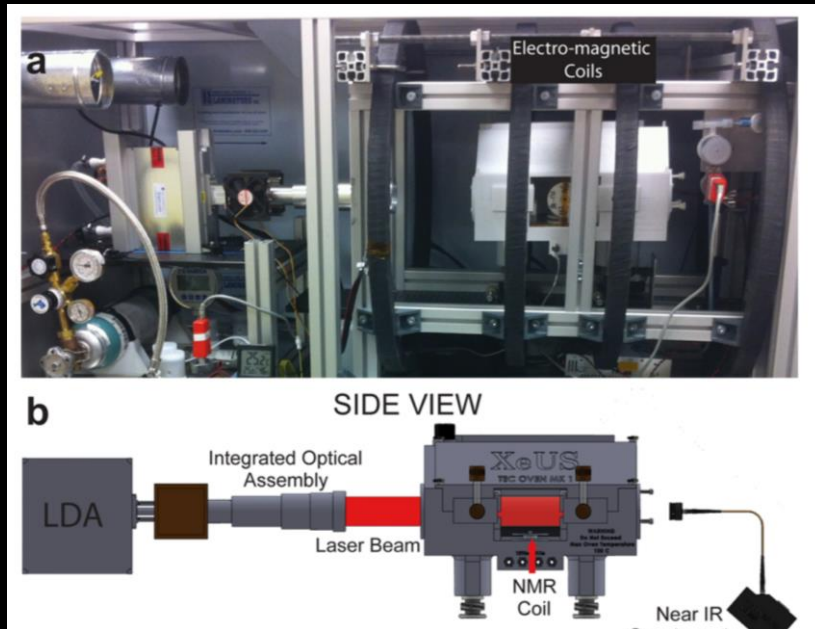


Other continuous-flow polarisers

Driehuys et al, APL(69), 1996; Haake et al., JACS(119), 1997; Rosen et al., RSI(70), 1999; Zook et al., JMR(159), 2002; Mortuza et al., JCP(118), 2003; Knagge et al., CPL(397), 2004; Schrank et al., PRA(80), 2009; Norquay et al., JAP(113), 2013. Korchak et al., AMR(44), 2013.

Two methods to polarise ^{129}Xe with spin-exchange optical pumping

Stopped-flow: ^{129}Xe polarised without cryogenic Xe accumulation



Birchall et al., AC(92), 2020.

Nikolaou et al., JPC(118), 2014.

Other stopped-flow polarisers

Birchall et al., Molecules(27), 2022; Raftery et al., PRL(66), 1991; Whiting et al., JMR(208), 2011; Six et al., PloS one(7), 2012; Hughes-Riley et al., JMR(237), 2013; Nikolaou et al., AC(86), 2014; Birchall et al., JMR(315), 2020.

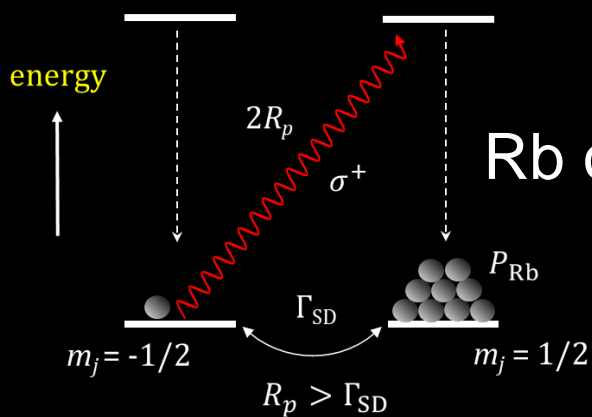
Stopped-flow vs continuous-flow

	Stopped-flow	Continuous-flow
Cryogenic separation of Xe	No	Yes
Xe in gas mix	>10%	1–3%
Laser powers	50–170	50–170
Typical ^{129}Xe polarisation	30%–95%	10%–50%
Xe production rates	100s ml/h	1000s ml/h
Low cell temp	$[\text{Rb}] \leq 10^{12} \text{ cm}^{-3}$	$[\text{Rb}] 10^{12} - 10^{14} \text{ cm}^{-3}$

Stopped-flow: Higher ^{129}Xe polarisations, lower Xe production rates

Continuous-flow: Lower ^{129}Xe polarisations, higher Xe production rates

Continuous-flow ^{129}Xe -Rb SEOP

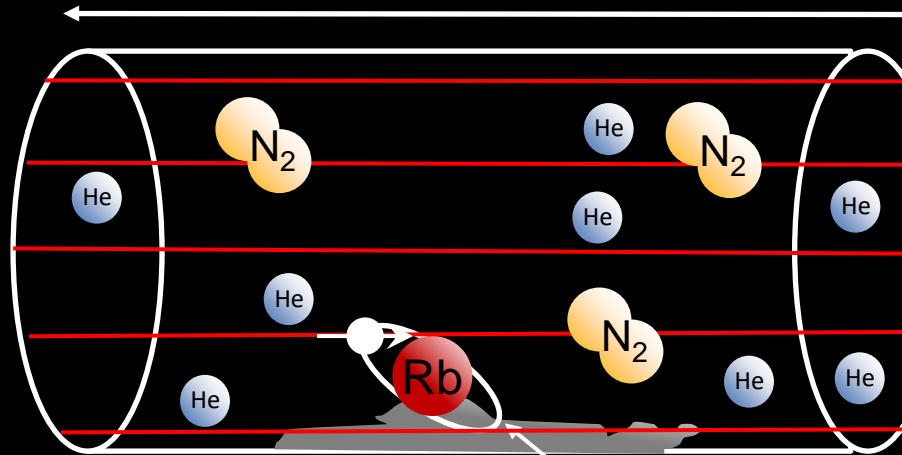


Need to purify – cryogenic separation...

$B_0 = 10-50$ G

- Circularly polarised light
- σ^+ helicity
- $\lambda_0 = 795$ nm

angular momentum



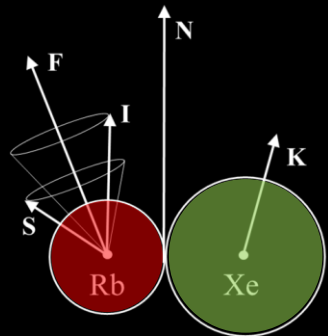
Incoming xenon

Bed of rubidium

Rb vapour density curve

$T > 40^\circ\text{C}$
(313.15 K)

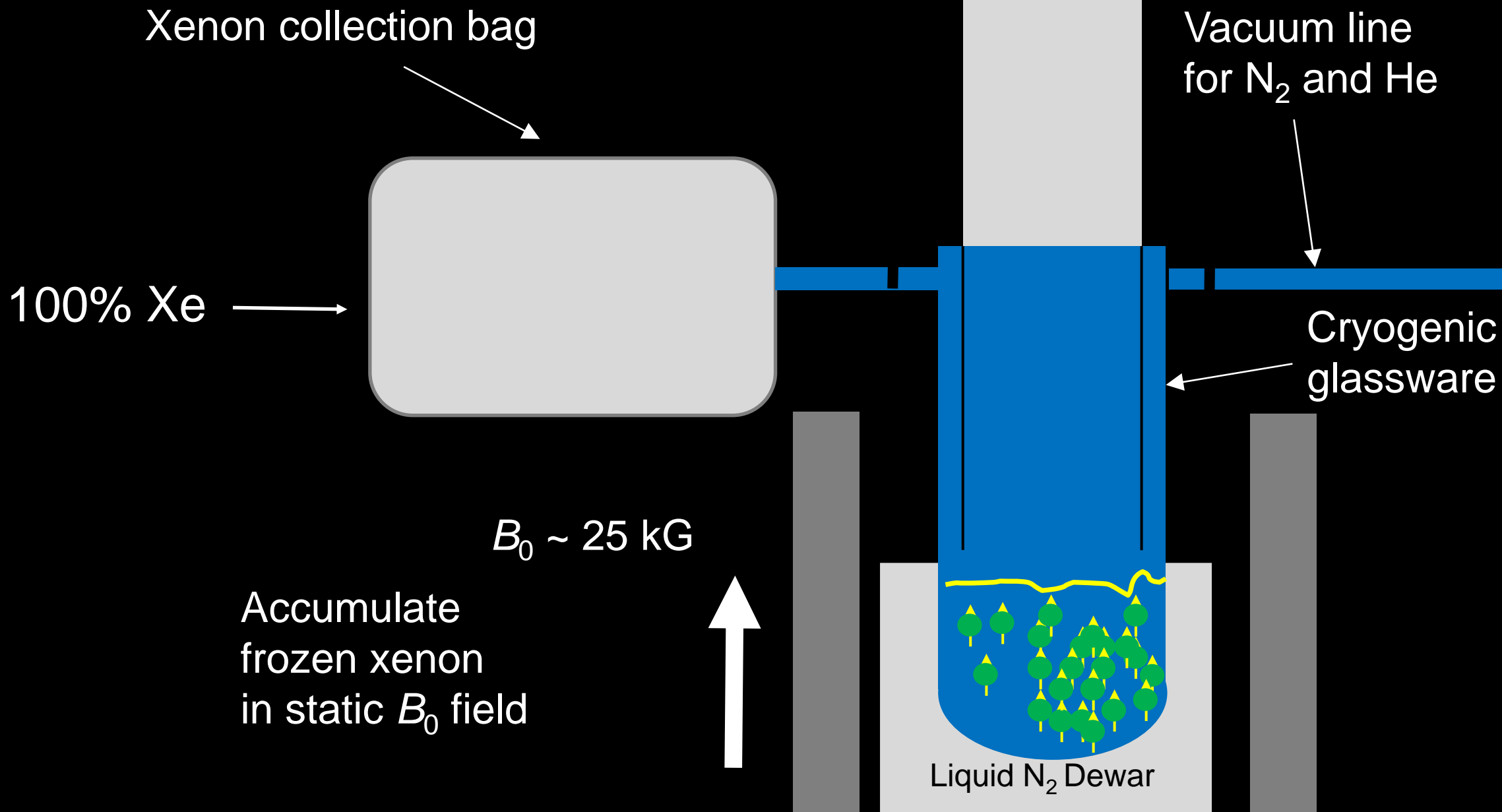
Path to cryogen



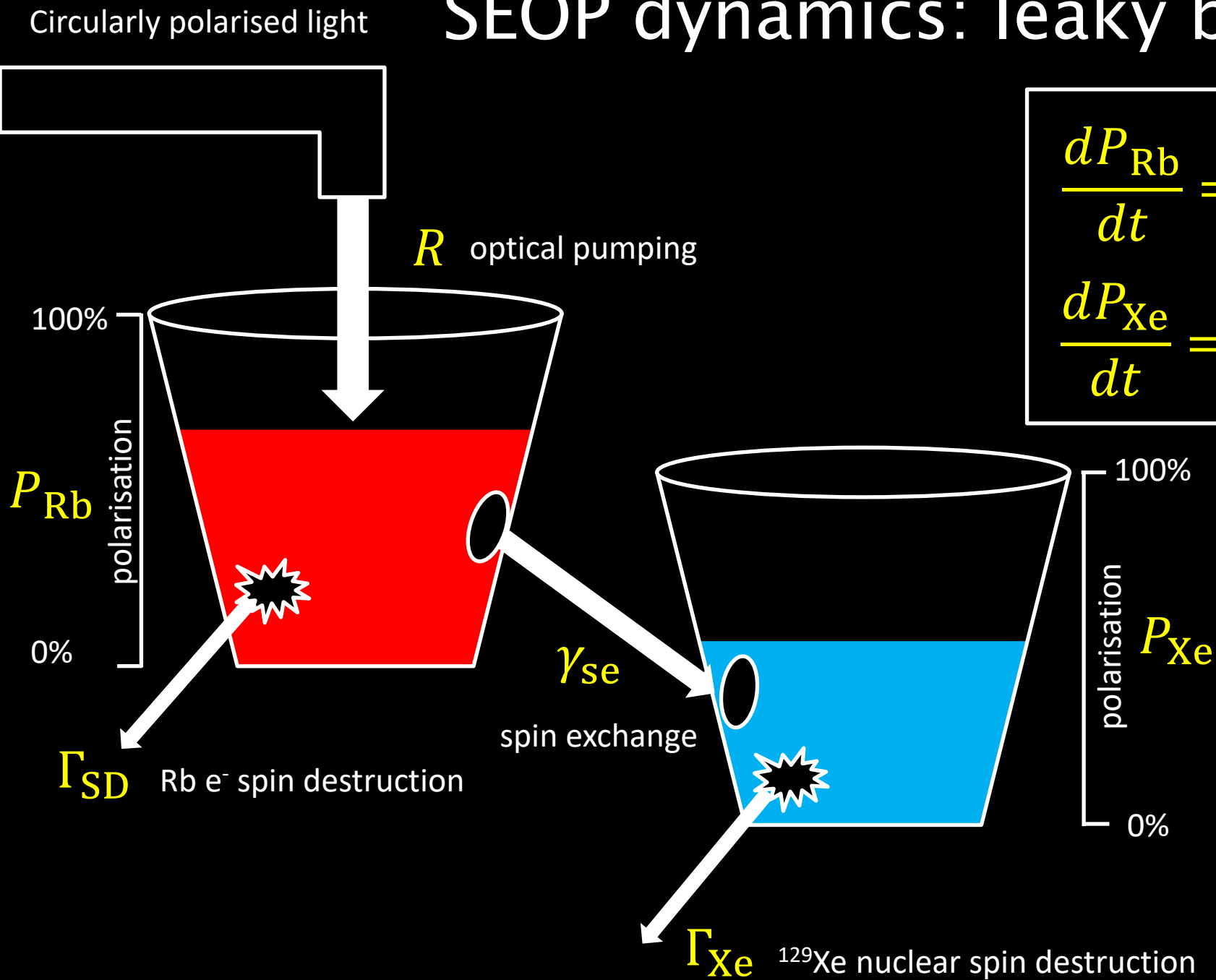
$$H = A\mathbf{I} \cdot \mathbf{S} + \gamma\mathbf{N} \cdot \mathbf{S} + \alpha\mathbf{K} \cdot \mathbf{S} + \dots$$

High Rb ^{129}Xe -Rb contact cross section

Freeze/thaw process



SEOP dynamics: leaky bucket model



$$\frac{dP_{Rb}}{dt} = (1 - P_{Rb})R - \Gamma_{SD}P_{Rb}$$

fill rate leak rate

$$\frac{dP_{Xe}}{dt} = \gamma_{se}(P_{Rb} - P_{Xe}) - \Gamma_{Xe}P_{Xe}$$

P_{Rb} and P_{Xe} time dependence

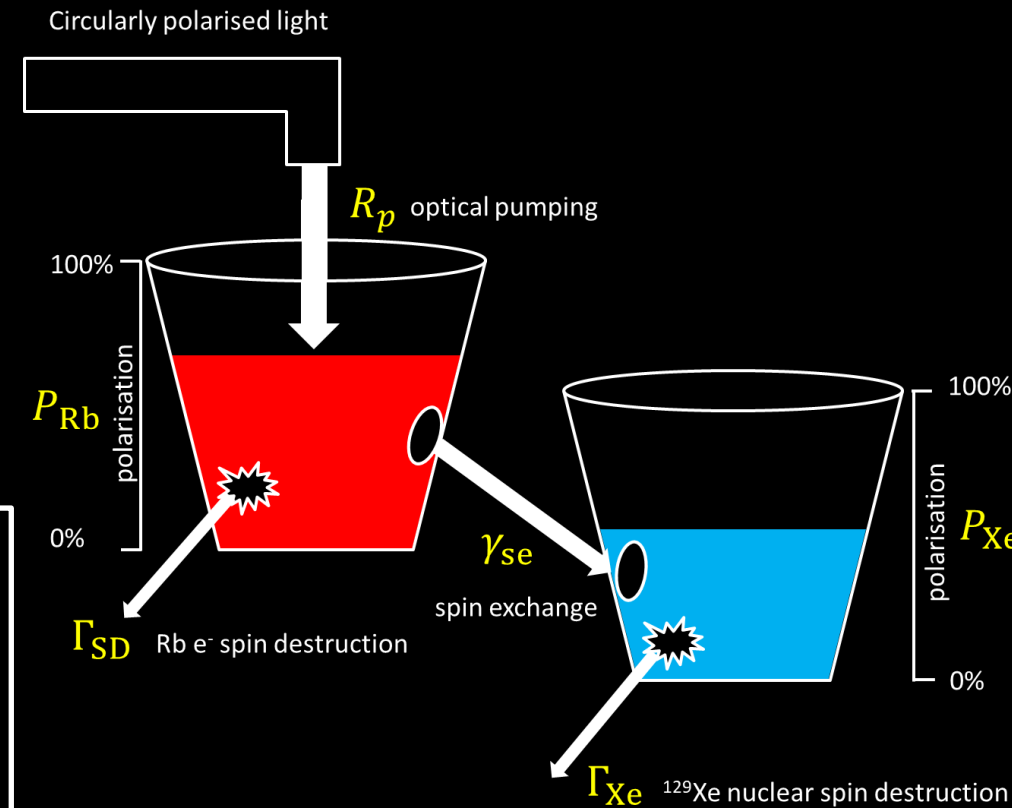
$$\frac{dP_{\text{Rb}}}{dt} = (1 - P_{\text{Rb}})R - \Gamma_{\text{SD}}P_{\text{Rb}}$$

$$\frac{dP_{\text{Xe}}}{dt} = \gamma_{\text{se}}(P_{\text{Rb}} - P_{\text{Xe}}) - \Gamma_{\text{Xe}}P_{\text{Xe}}$$

$$P_{\text{Rb}}(t) = \frac{R}{R + \Gamma_{\text{SD}}} (1 - e^{-(R + \Gamma_{\text{SD}})t})$$

$$P_{\text{Xe}}(t) = \frac{\gamma_{\text{se}}}{\gamma_{\text{se}} + \Gamma_{\text{Xe}}} P_{\text{Rb}}(t) (1 - e^{-(\gamma_{\text{se}} + \Gamma_{\text{Xe}})t})$$

Leaky bucket model



P_{Rb} and P_{Xe} steady-state and build up

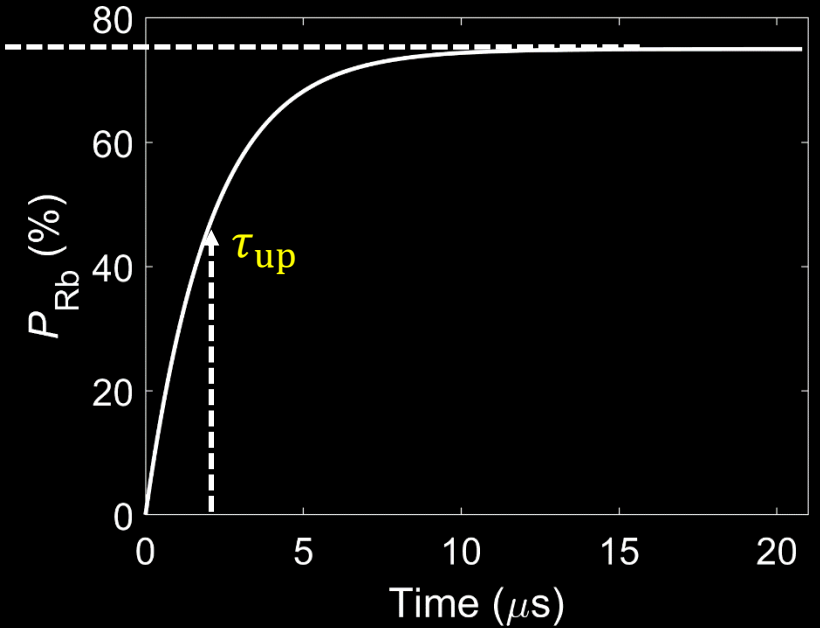
Rb polarisation

$$P_{\text{Rb}}(t) = \frac{R}{R + \Gamma_{\text{SD}}} \left(1 - e^{-(R_p + \Gamma_{\text{SD}})t} \right)$$

$$\text{Steady-state: } P_{\text{Rb}} = \frac{R}{R + \Gamma_{\text{SD}}}$$

$$\text{Spin-up time: } \tau_{\text{up}} = 1/(R_p + \Gamma_{\text{SD}}) \approx \text{micro seconds}$$

$$\frac{R}{R + \Gamma_{\text{SD}}}$$



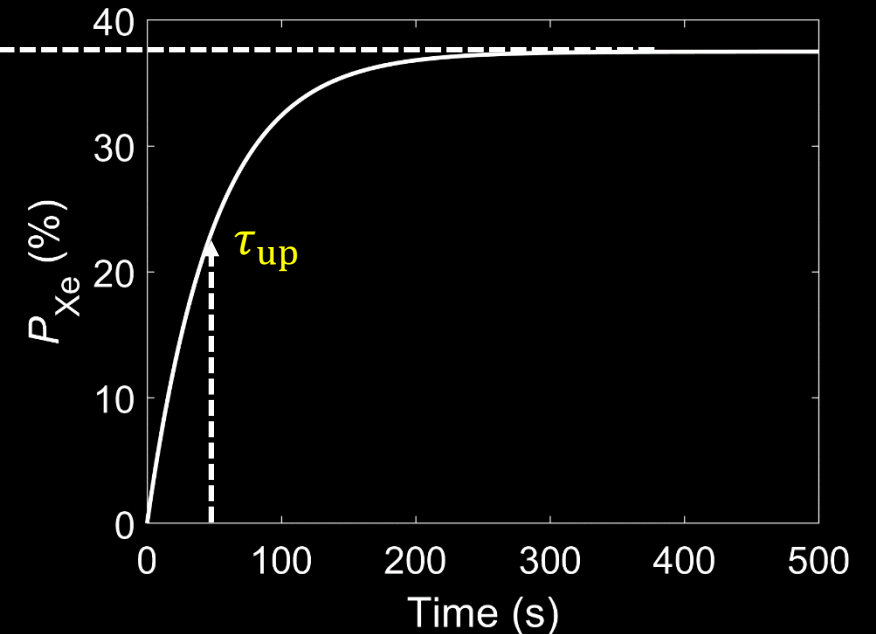
^{129}Xe polarisation

$$P_{\text{Xe}}(t) = \frac{\gamma_{\text{se}}}{\gamma_{\text{se}} + \Gamma_{\text{Xe}}} P_{\text{Rb}}(t) \left(1 - e^{-(\gamma_{\text{se}} + \Gamma_{\text{Xe}})t} \right)$$

$$\text{Steady-state: } P_{\text{Xe}} = \frac{\gamma_{\text{se}}}{\gamma_{\text{se}} + \Gamma_{\text{Xe}}} P_{\text{Rb}}$$

$$\text{Spin-up time: } \tau_{\text{up}} = 1/(\gamma_{\text{se}} + \Gamma_{\text{Xe}}) \approx \text{10s of seconds}$$

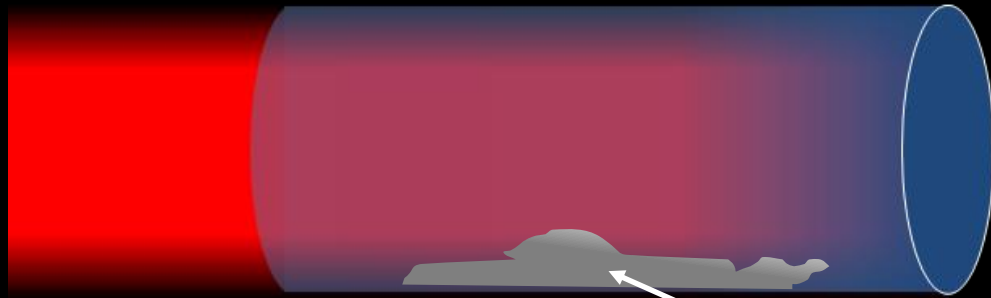
$$\frac{\gamma_{\text{se}}}{\gamma_{\text{se}} + \Gamma_{\text{Xe}}} P_{\text{Rb}}$$



Light propagation: spatial dependence

Photon flux Φ

→ z



Rb pool

$$\frac{\partial \Phi(\nu, z)}{\partial z} = -\underbrace{\lambda^{-1}(\nu, z)}_{\text{absorption length per photon}} \Phi(\nu, z)$$

λ = absorption length
per photon

$$\lambda^{-1}(\nu, z) = [\text{Rb}] \sigma(\nu) [1 - P_{\text{Rb}}(z)]$$

↑
Rb vapour density

← Rb polarisation

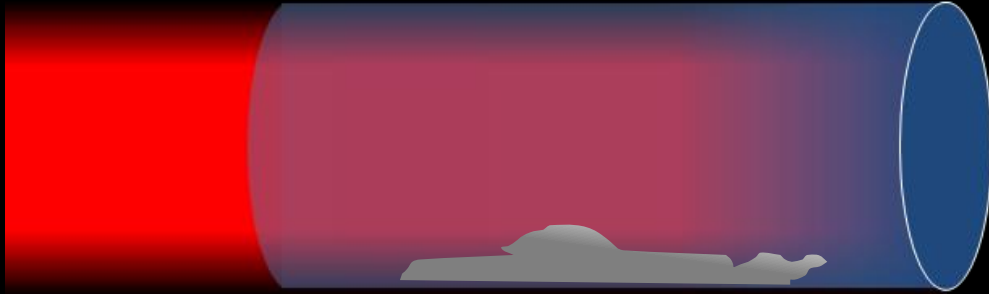
← Rb D1 line absorption profile

$$\frac{\partial \Phi(\nu, z)}{\partial z} = -[\text{Rb}] \sigma(\nu) [1 - P_{\text{Rb}}(z)] \Phi(\nu, z)$$

Absorption profile over cell length

Photon flux Φ

→ z

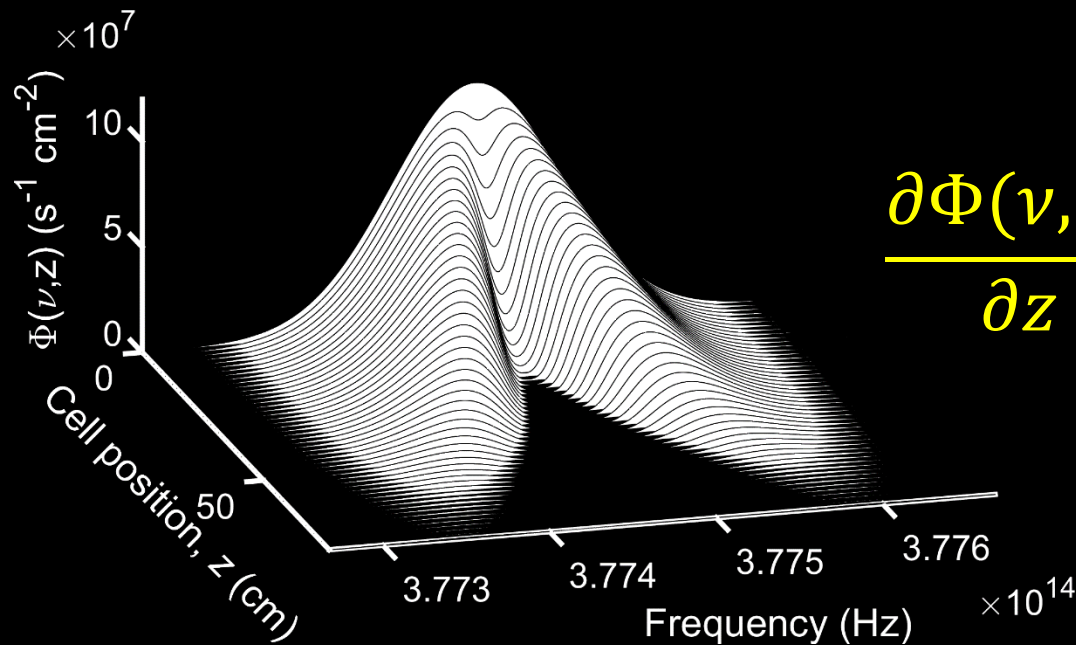


Incident flux

$$\Phi(\nu, 0) = \Phi_0 \exp \left[-4 \ln 2 \frac{(\nu - \nu_l)^2}{\Delta\nu_l^2} \right] \quad \text{Gaussian}$$

Absorption

$$\sigma(\nu) = \sigma_0 \frac{\Delta\nu_a/2\pi}{(\nu - \nu_a)^2 + \left(\frac{\Delta\nu_a}{2}\right)^2} \quad \text{Lorentzian}$$



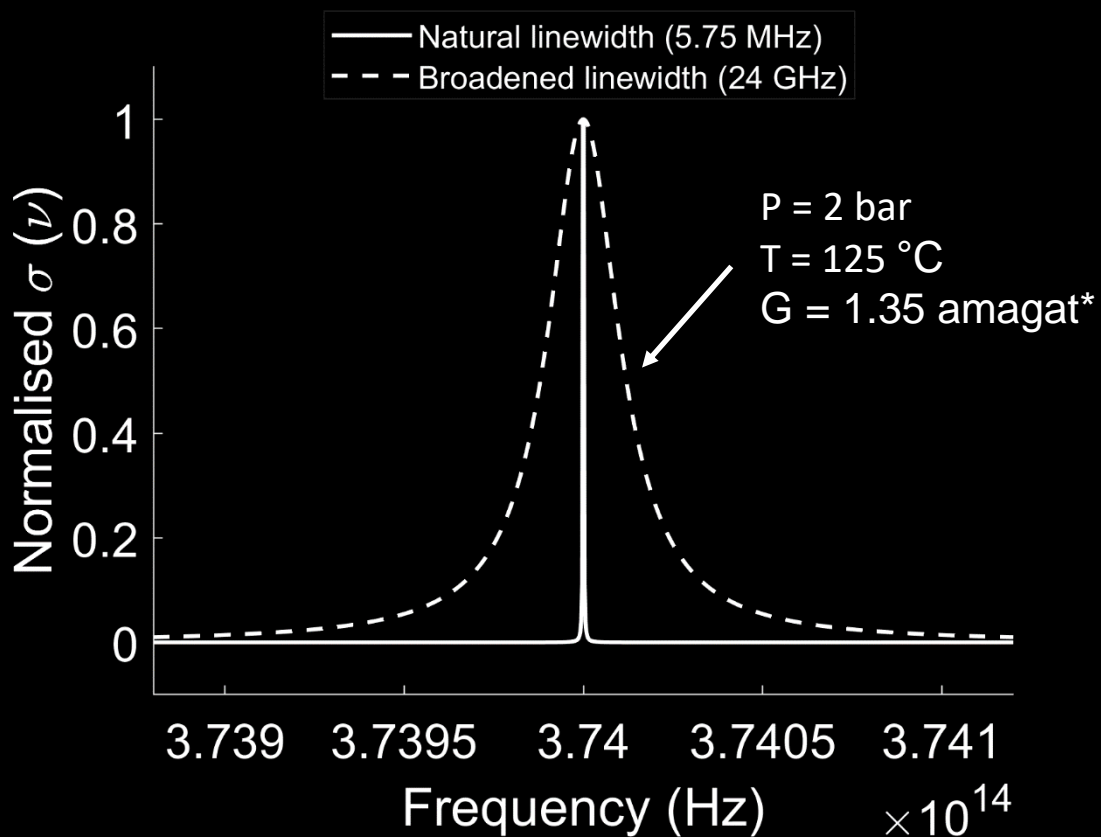
$$\frac{\partial \Phi(\nu, z)}{\partial z} = -[\text{Rb}] \sigma(\nu) [1 - P_{\text{Rb}}(z)] \Phi(\nu, z)$$

$$\Delta\nu_l = 142 \text{ GHz (0.30 nm)}$$

$$\Delta\nu_a = 24 \text{ GHz (0.05 nm)}$$

Role of buffer gases N₂ and He

Pressure broadening of D₁ line

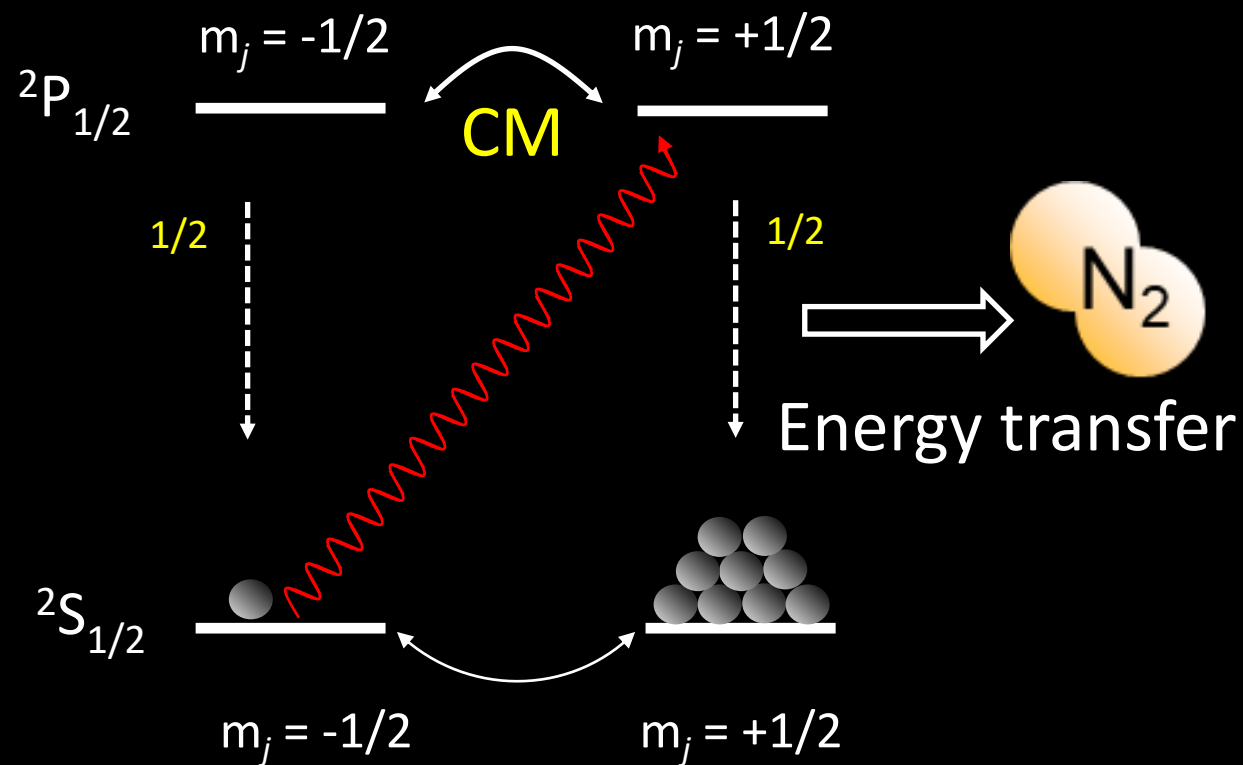


He/N₂ : $\Delta\nu_a \sim 18 \text{ GHz/amagat}$

Romalis, PRA(56), 1997

*1 amagat = gas number density at STP ($T = 0^\circ\text{C}$ and $P = 1 \text{ atm}$)

Non-radiative decay (quenching)



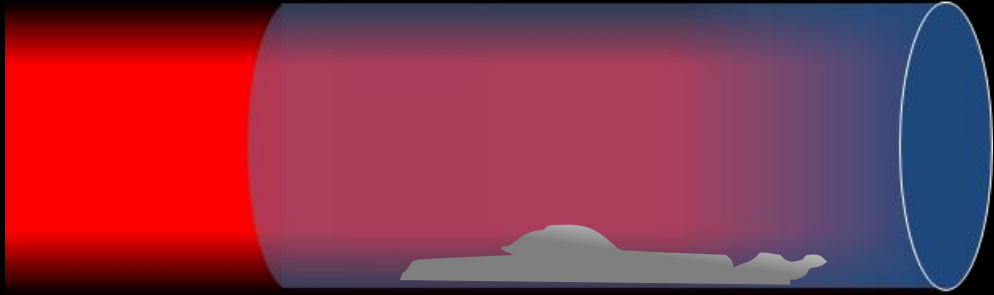
CM = collisional mixing

Wagshul and Chupp, PRA(40), 1989

Light propagation and optical pumping

Photon flux Φ

→ z



$$R(z) = \int \Phi(\nu, z) \sigma(\nu) d\nu$$

Optical pumping rate

$$\frac{\partial \Phi(\nu, z)}{\partial z} = -[\text{Rb}] \sigma(\nu) [1 - P_{\text{Rb}}(z)] \Phi(\nu, z)$$

$$\frac{d\Phi(z)}{dz} = \int \frac{\partial \Phi(z, \nu)}{\partial z} d\nu = -[\text{Rb}] [1 - P_{\text{Rb}}(z)] \int \Phi(\nu, z) \sigma(\nu) d\nu$$

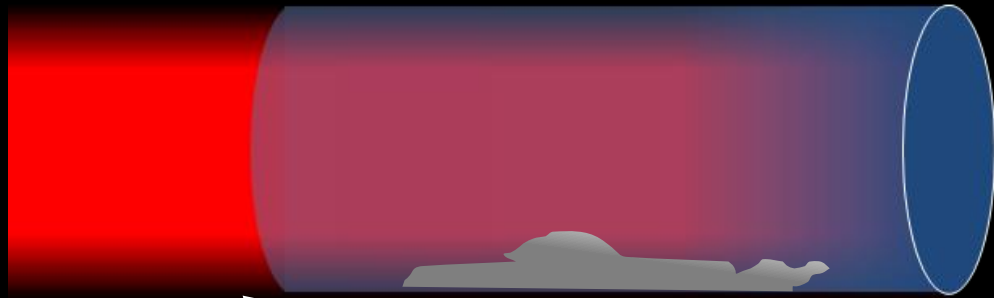
$$\frac{d\Phi(z)}{dz} = -[\text{Rb}] [1 - P_{\text{Rb}}(z)] R(z)$$

Relates photon attenuation
with pumping rate

Optical pumping rate vs cell length

Photon flux Φ

$\longrightarrow z$



$$\frac{d\Phi(z)}{dz} = -[\text{Rb}][1 - P_{\text{Rb}}(z)]R(z)$$

$$R_0(\nu, 0) = \int_{-\infty}^{\infty} \sigma(\nu)\Phi(\nu) = \alpha\Phi$$

$$\alpha = \frac{2\sqrt{\pi \ln 2} r_e f \lambda_l^3 w'(r, s)}{hc\Delta\lambda n_p}$$

Appelt, PRA(52), 1998

$$\frac{dR(z)}{dz} = -[\text{Rb}]\alpha[1 - P_{\text{Rb}}(z)]R(z)$$

$$W(f(x)) = x, \text{ for } f(x) = xe^x$$

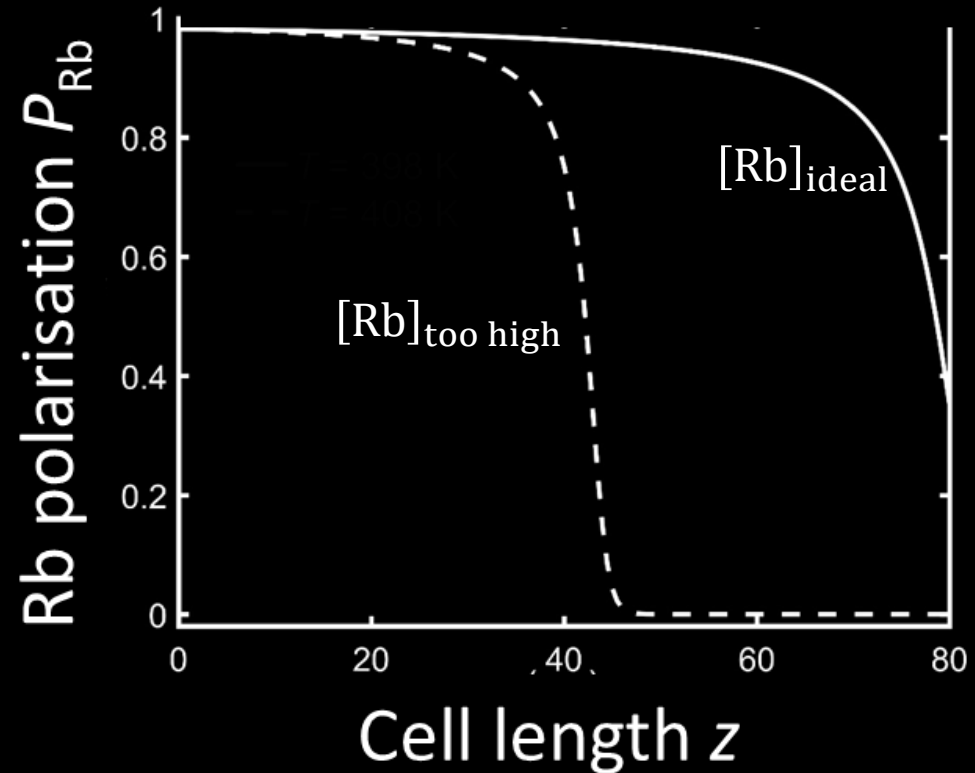
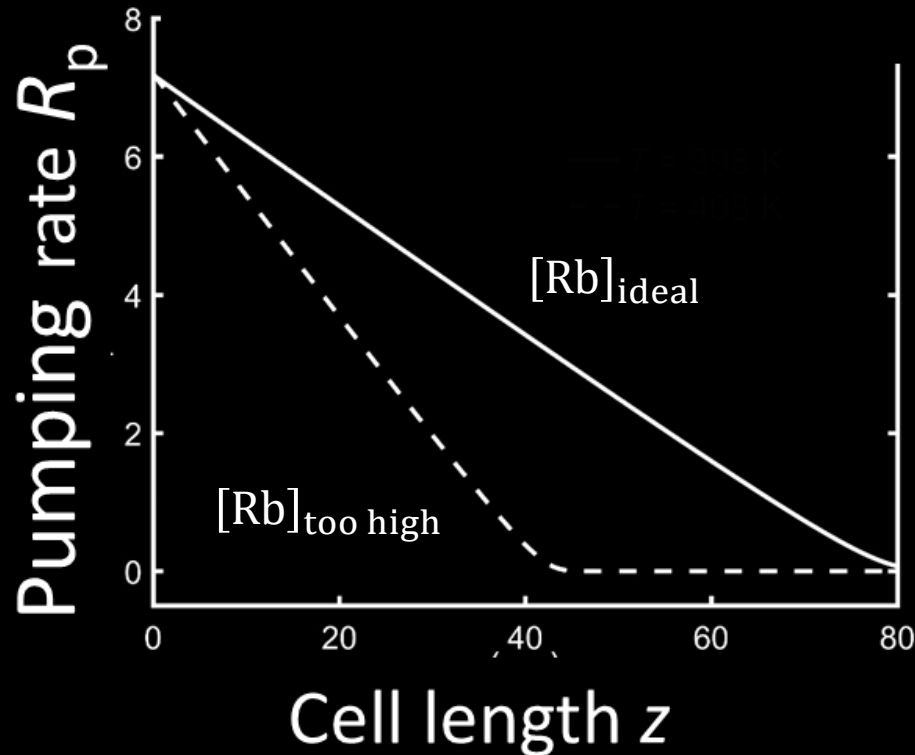
$$R(z) = \Gamma_{SD} W \left(\frac{R_0}{\Gamma_{SD}} \exp \left(\frac{R_0}{\Gamma_{SD}} - \alpha[\text{Rb}]z \right) \right)$$

Product log
function

Optimisation tools: Light propagation, R_p and P_{Rb}

$$R(z) = \Gamma_{SD} W \left(\frac{R_0}{\Gamma_{SD}} \exp \left(\frac{R_0}{\Gamma_{SD}} - \alpha [\text{Rb}] z \right) \right)$$

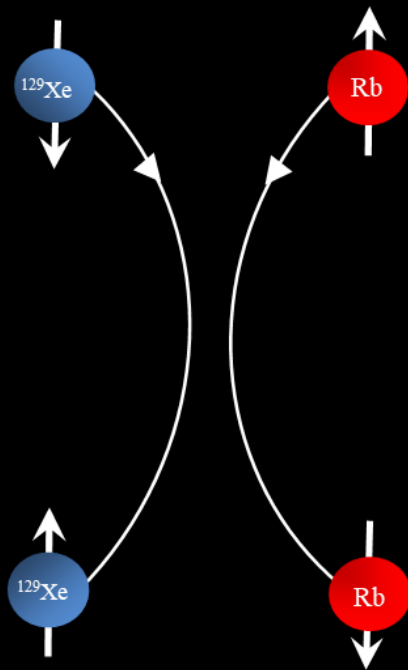
$$P_{Rb}(z) = \frac{R(z)}{R(z) + \Gamma_{SD}}$$



Solid white line necessary for high average P_{Rb} over the cell volume

^{129}Xe -Rb spin exchange

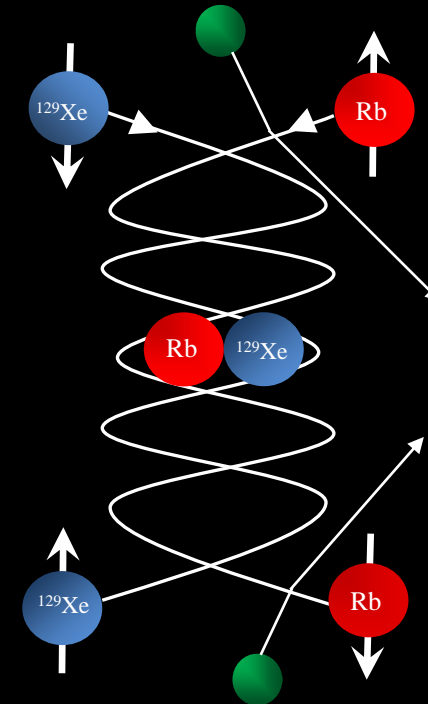
Two-body collisional exchange



- Simple two-body cross section
- Independent of P_{Rb} and gas composition

Three-body vdW molecular exchange

3rd body {N₂, He, Xe}



- Complicated cross section
- Depends on P_{Rb} and gas composition

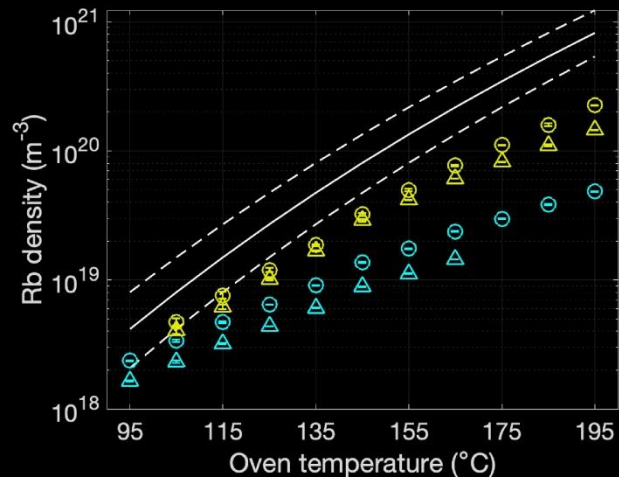
^{129}Xe -Rb spin exchange

Two-body collisional exchange

$$\gamma_{se}^{bc} = \langle \sigma v \rangle [\text{Rb}]$$

Binary spin-exchange cross section

Ball et al, Molecules(8), 2023



Factor-2 lower [Rb] than standard saturation curves

$$\gamma' = \langle \sigma v \rangle + \gamma'_{vdW} = 1.2 \times 10^{-21} \text{ cm}^3 \text{ s}^{-1}$$

Literature: $\langle \sigma v \rangle = 0.1 \times 10^{-21}$ to $1 \times 10^{-21} \text{ cm}^3 \text{ s}^{-1}$

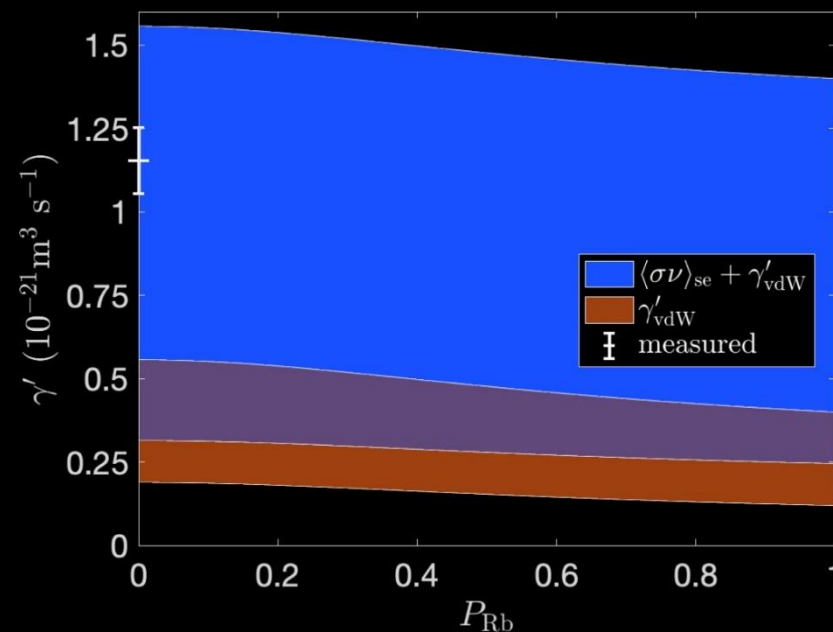
Factor-10 range in values...

Three-body vdW molecular exchange

$$\gamma_{se}^{vdw} = \frac{1}{2T_K} \left(\frac{\omega_{sr}\tau}{x} \right)^2 \sum_i \eta_i \left(\frac{1 + q_i(\omega_{h,i}\tau)^2/[I_i]^2}{1 + (\omega_{h,i}\tau)^2} \right) = \gamma'_{vdW} [\text{Rb}]$$

τ = molecular lifetime ← Gas composition dependent

$q_i = 1 + \epsilon(I, P_{\text{Rb}})$ ← Nuclear slowing down factor

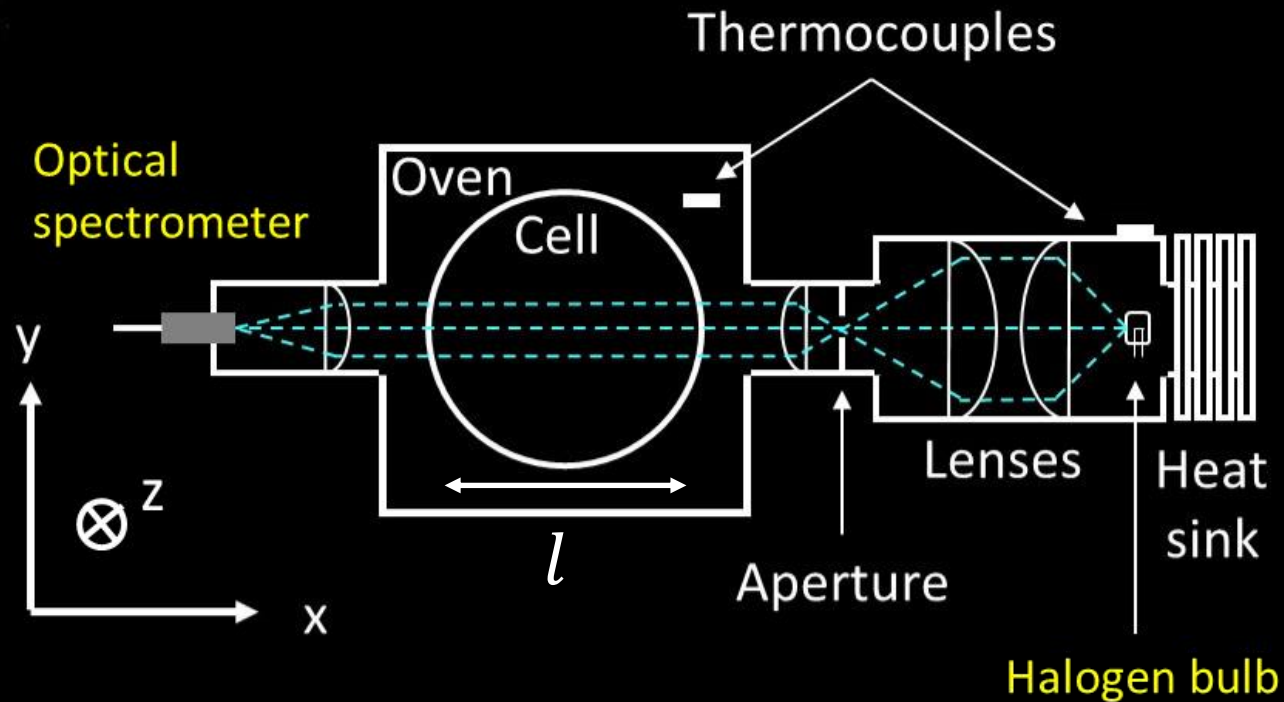


Ball et al, Molecules(8), 2023

Measuring Rb vapour density

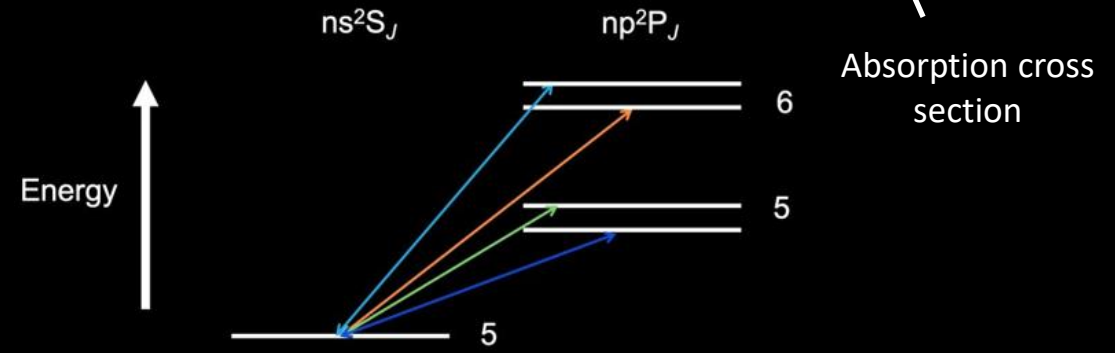
Atomic Absorption spectroscopy

Experimental Set up



Beer-Lambert law

$$I(\nu) = I_0 e^{-[\text{Rb}]\sigma(\nu)l}$$



Transition	Wavelength (nm)	Oscillator strength, f
$5^2S_{1/2} \rightarrow 6^2P_{1/2}$	422	3.87×10^{-3}
$5^2S_{1/2} \rightarrow 6^2P_{3/2}$	420	9.46×10^{-3}
$5^2S_{1/2} \rightarrow 5^2P_{1/2} (D_1)$	795	3.422×10^{-1}
$5^2S_{1/2} \rightarrow 5^2P_{3/2} (D_2)$	780	6.957×10^{-1}

Measuring Rb vapour density

Atomic Absorption spectroscopy

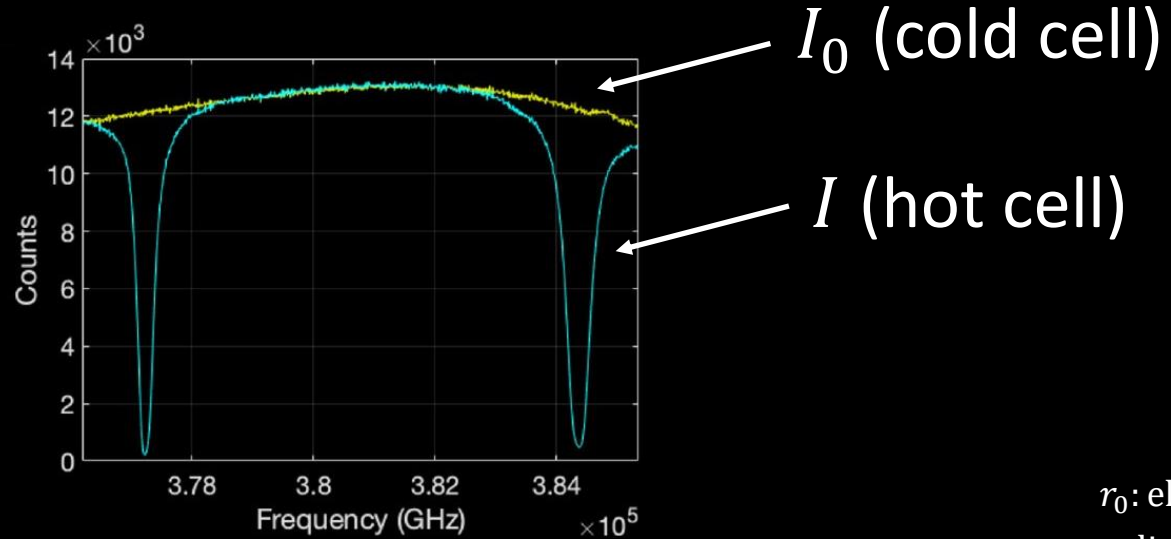
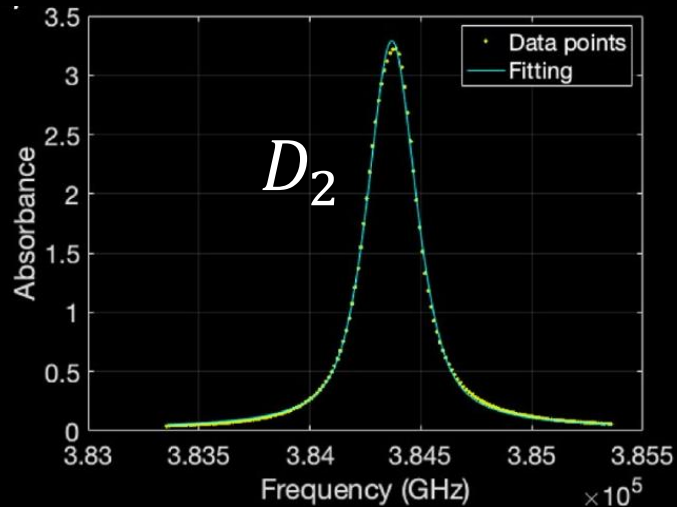
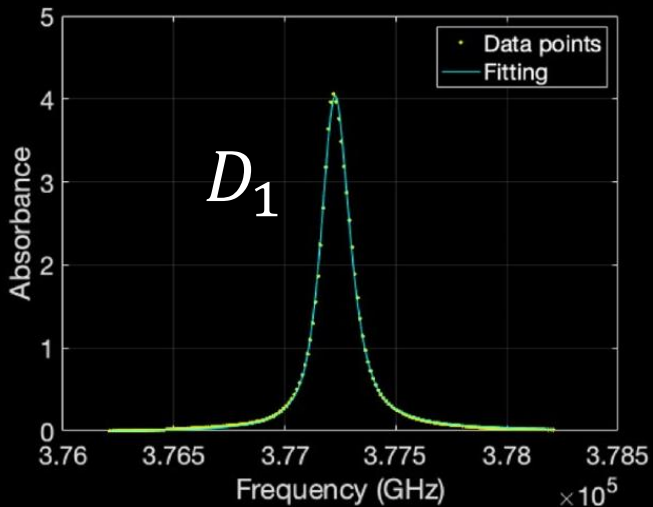
$$I = I_0 e^{-[\text{Rb}]\sigma(\nu)l}$$

Absorbance

Amplitude

$$S(\nu) = \ln\left(\frac{I_0}{I}\right) = AL(\nu)$$

Normalised Lorentzian



Transition oscillator strength

r_0 : electron radius
 c : light speed

$$[\text{Rb}] = \frac{1}{\sigma_0 l} \int S(\nu) d\nu$$

$$\sigma_0 = \int \sigma(\nu) d\nu = \pi r_0 c f$$

$$[\text{Rb}] = \frac{A}{\pi r_0 c f l}$$

Optimisation tools: ^{129}Xe polarisation

$$P_{\text{Xe}}(t_{\text{res}}) = \frac{\gamma_{\text{se}}}{\gamma_{\text{se}} + \Gamma_{\text{Xe}}} \langle P_{\text{Rb}} \rangle [1 - e^{-t_{\text{res}}/\tau_{\text{up}}}]$$

mean Rb polarisation over cell volume

Xe cell residency time

$\gamma_{\text{se}} = \gamma_{\text{se}}^{bc} + \gamma_{\text{se}}^{vdW}$

^{129}Xe spin-exchange rate

^{129}Xe spin-destruction rate

^{129}Xe spin-up time

$\gamma_{\text{se}} \propto [\text{Rb}]$

$\Gamma_{\text{Xe}} = 1/T_1$

$\tau_{\text{up}} = 1/(\gamma_{\text{se}} + \Gamma_{\text{Xe}})$

For high P_{Xe} :

$$\gamma_{\text{se}} > 1/T_1 \quad \text{High } \langle P_{\text{Rb}} \rangle \quad t_{\text{res}} > \tau_{\text{up}}$$

Continuous-flow polariser optimisation

Rationale for a large cell

- Long cell maximises absorption of incident photons at lower [Rb]
- Laser heating/Rb runaway less likely
- At high gas flow rate Q and lower [Rb]
 $t_{\text{res}} > \tau_{\text{up}}$ for large volume cell



$$t_{\text{res}} = \frac{[G]V_{\text{cell}}}{Q} \quad \tau_{\text{up}} \propto 1/[Rb]$$

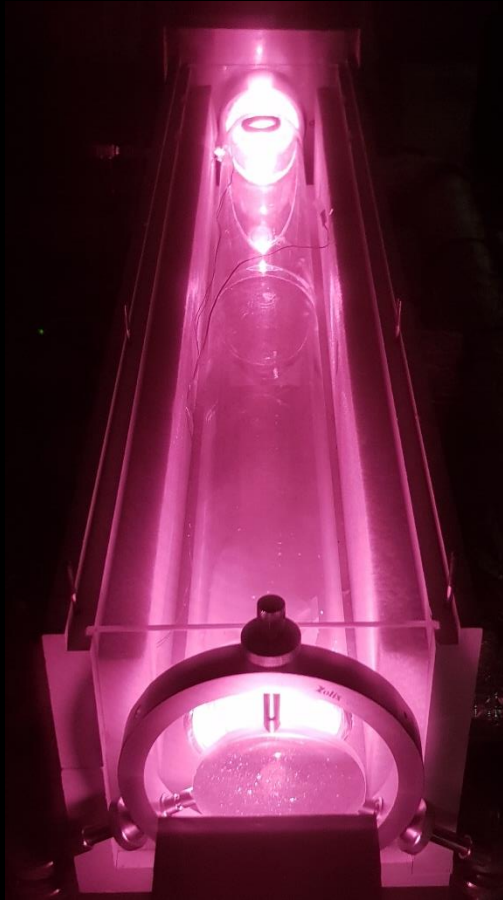
High P_{Xe} at rapid Xe production rates

Polariser design: **large-volume optical cell**

$$P_{Xe}(t_{res}) = P_0(1 - e^{-t_{res}/\tau_{up}})$$

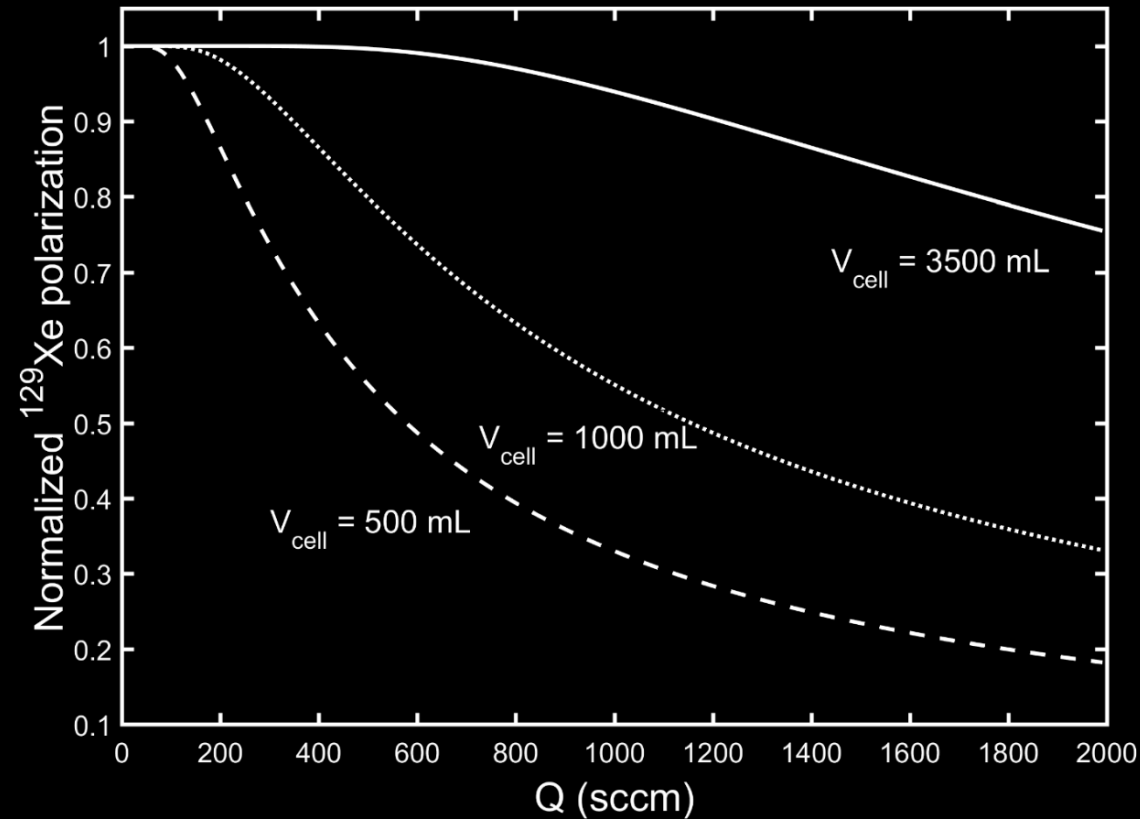
$$P_{Xe}(Q) = P_0(1 - e^{-[G]V_{cell}/Q\tau_{up}})$$

$$t_{res} = \frac{[G]V_{cell}}{Q}$$



Cell dimensions:

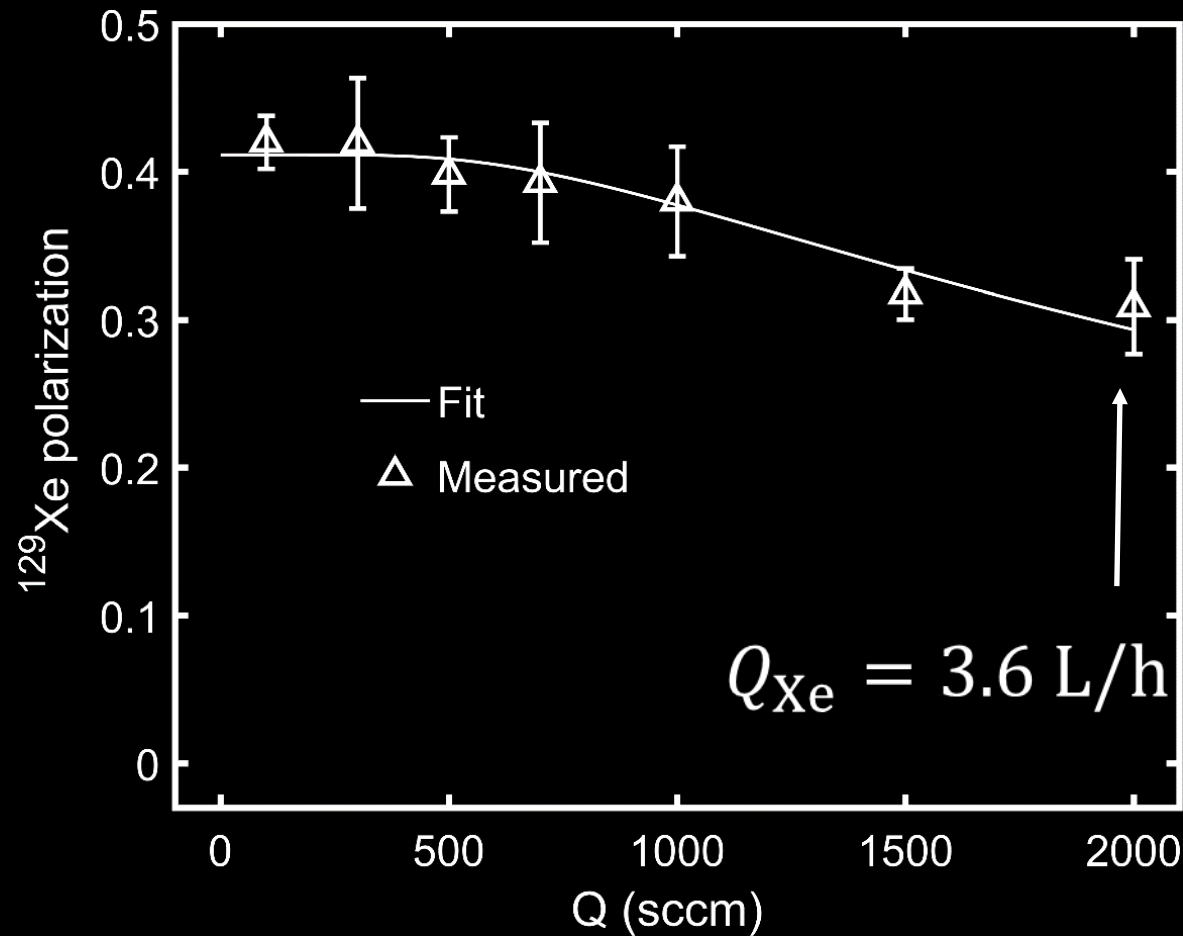
- Length = 80cm
- Diameter = 7.5 cm
- Volume = 3530 mL



Simulated:

- $T_{cell} = 398 \text{ K}$
- $P_{cell} = 1.25 \text{ bar}$
- $[G] = 0.85 \text{ amg}$

^{129}Xe polariser optimisation



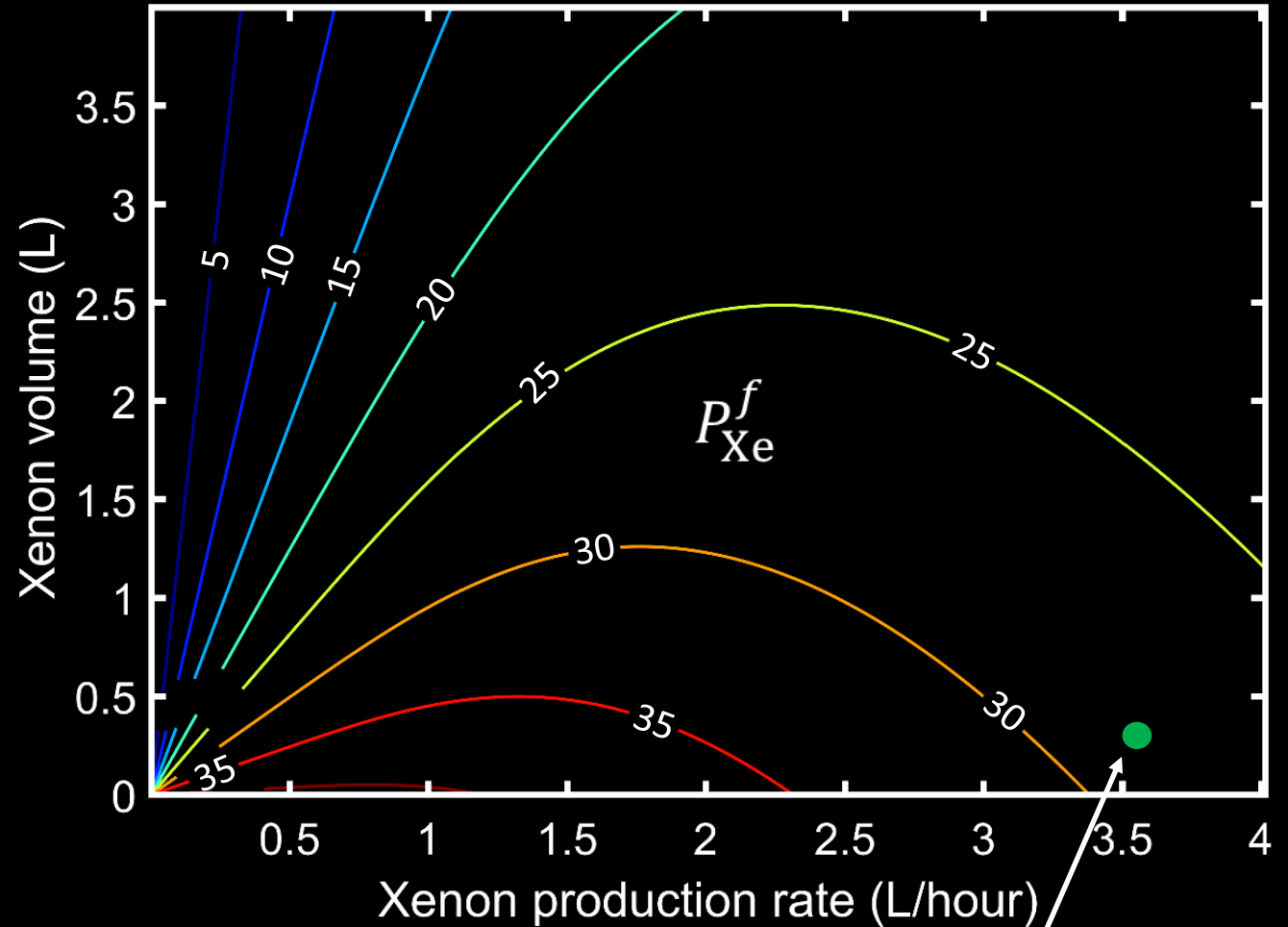
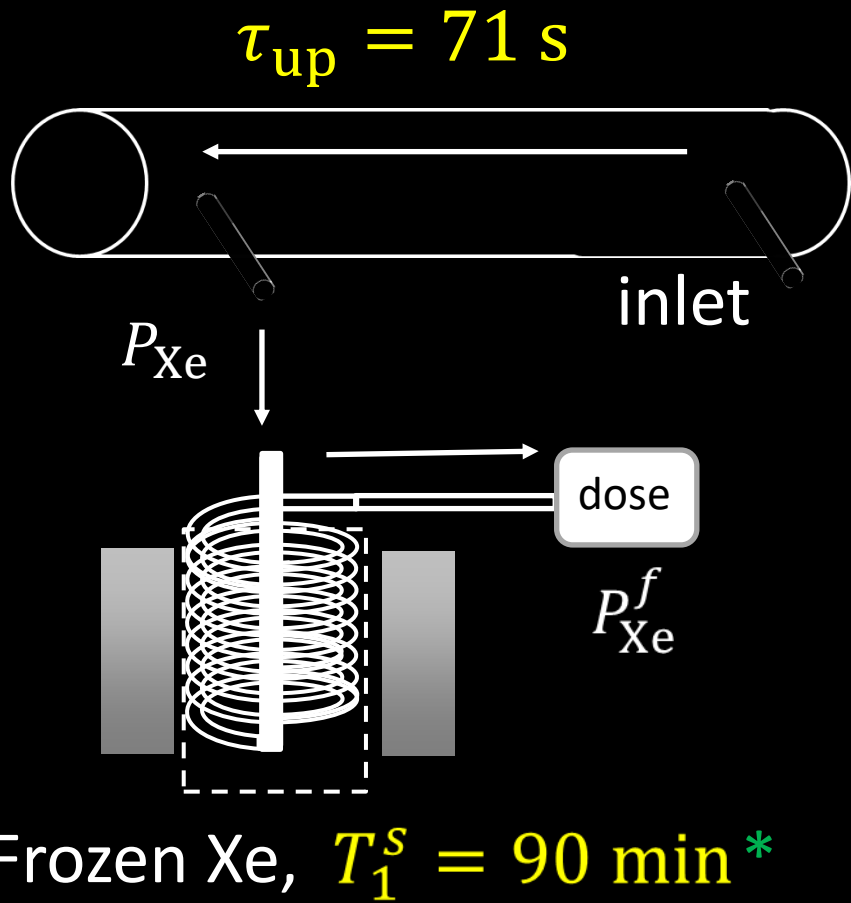
Optimised parameters:

- $T_{\text{cell}} = 398 \text{ K}$
- $P_{\text{cell}} = 1.25 \text{ bar}$
- 3% Xe gas mix
- $[G] = 0.85 \text{ amg}$
- $V_{\text{cell}} = 3530 \text{ mL}$

$$Q = 2000 \text{ sccm} \Rightarrow t_{\text{res}} = 90 \text{ s}$$

$$P_{\text{Xe}}(Q) = P_0(1 - e^{[G]V_{\text{cell}}/Q\tau_{\text{up}}}) \Rightarrow \tau_{\text{up}} = 71 \text{ s} \Rightarrow P(Q = 2000) \approx 0.75P_0$$

^{129}Xe production map



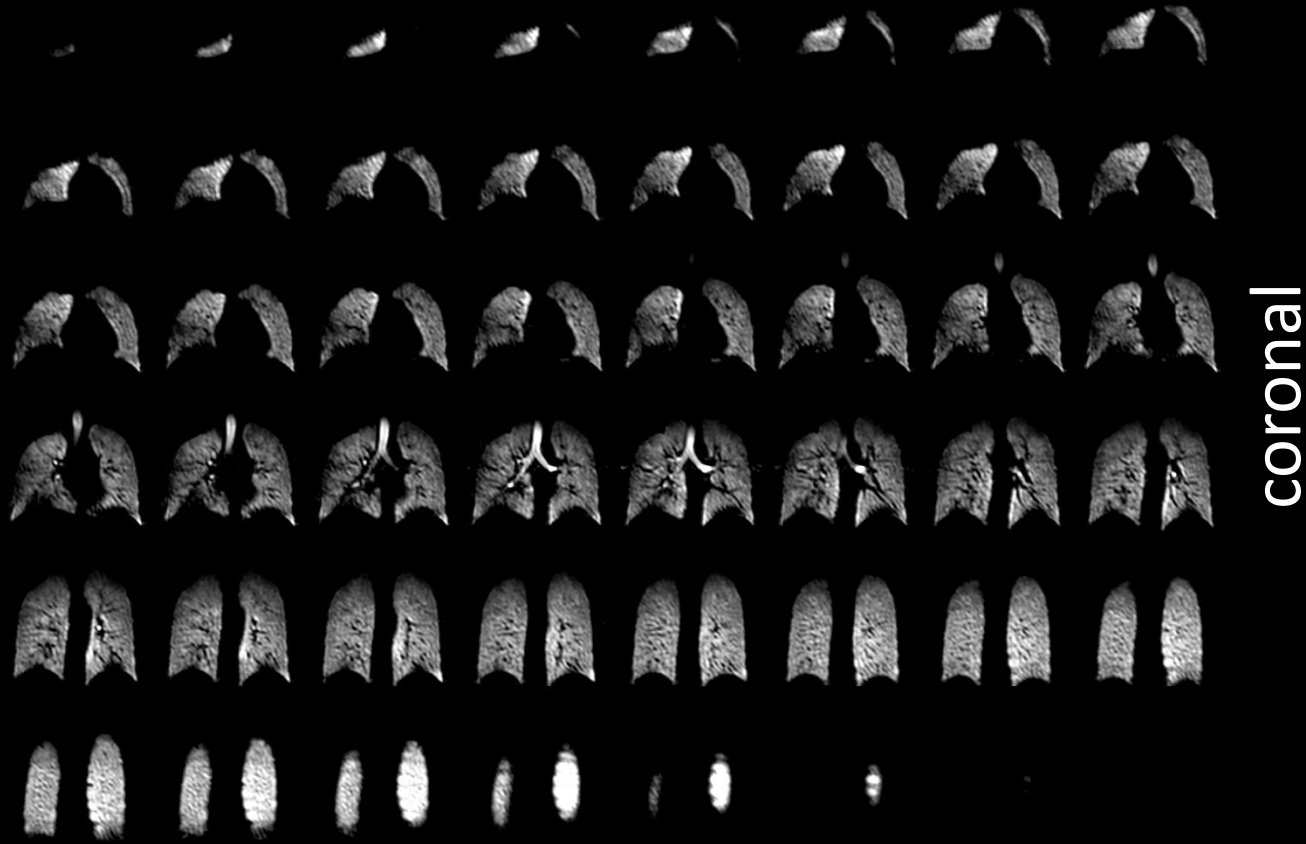
300 mL, $P_{\text{Xe}} \sim 30\%$ in 5 min

$$P_{\text{Xe}}^f(Q, t_a) = P_{\text{Xe}}(Q) \left[1 - e^{-t_a/T_1^s} \right] T_1^s / t_a$$

*Norquay et al., J Appl Phys(13), 2013

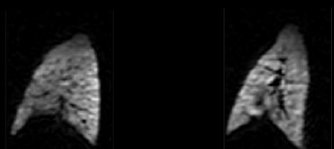
Norquay et al., Phys Rev Lett(121), 2018

3D ^{129}Xe human lung imaging with enriched Xe



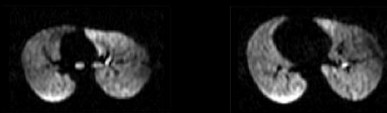
coronal

Enriched Xe:
1L dose generated
~20 min



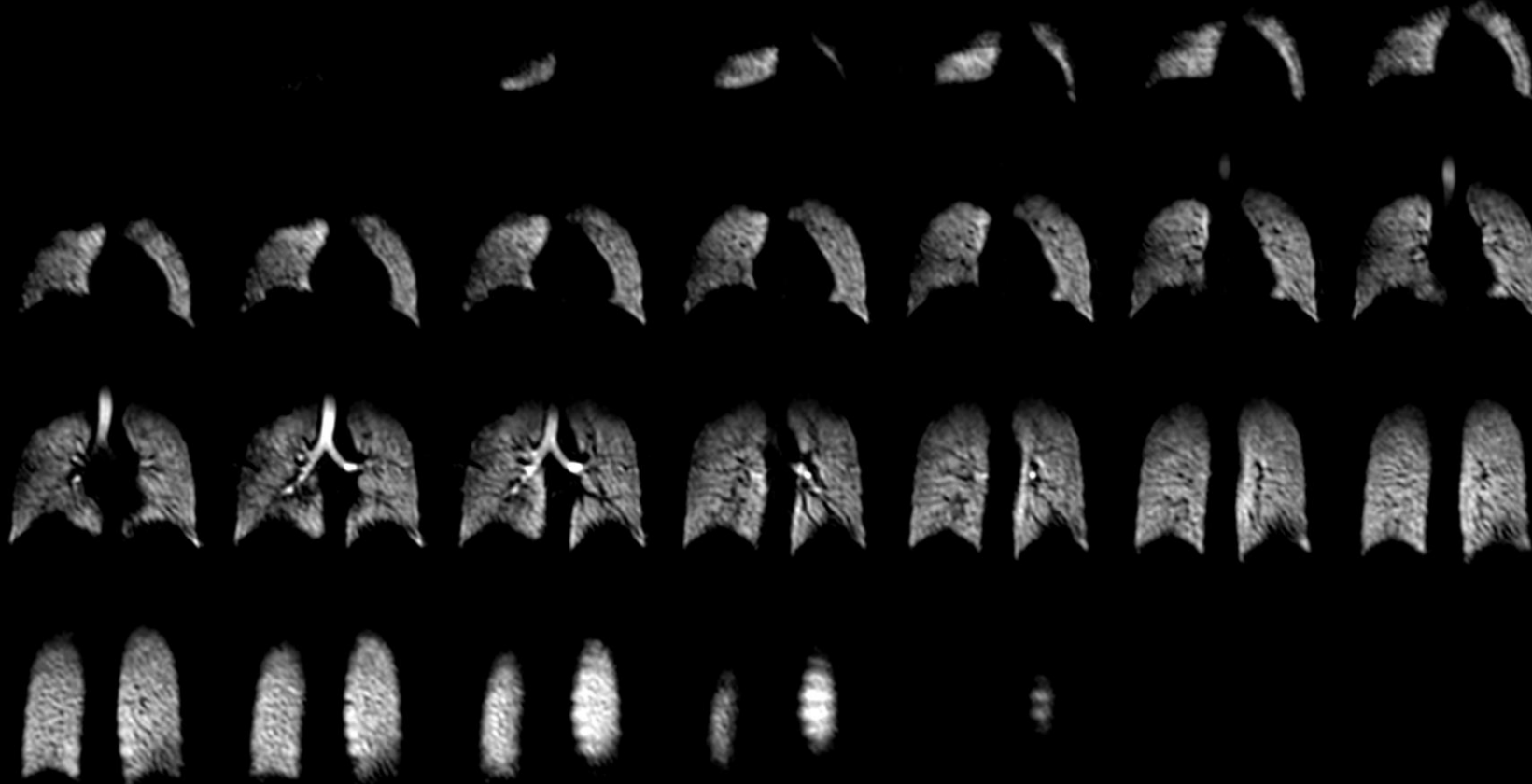
sagittal

Isotropic
resolution:
4.2 mm³



axial

3D ^{129}Xe human lung imaging with NA Xe

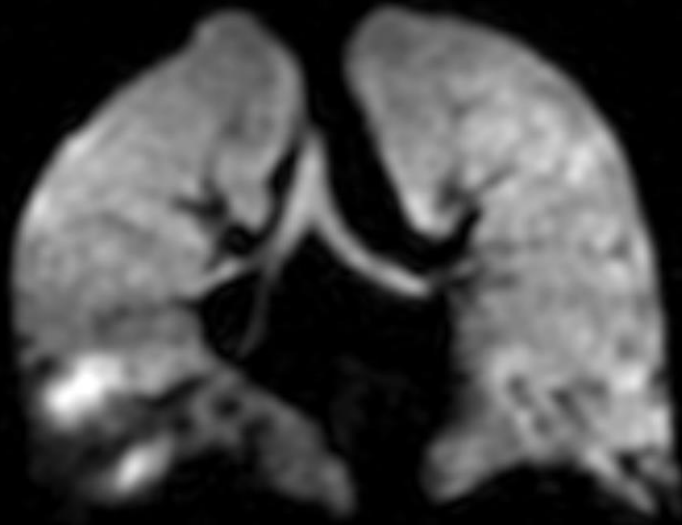


\$25/scan
1/8 cost of enriched Xe

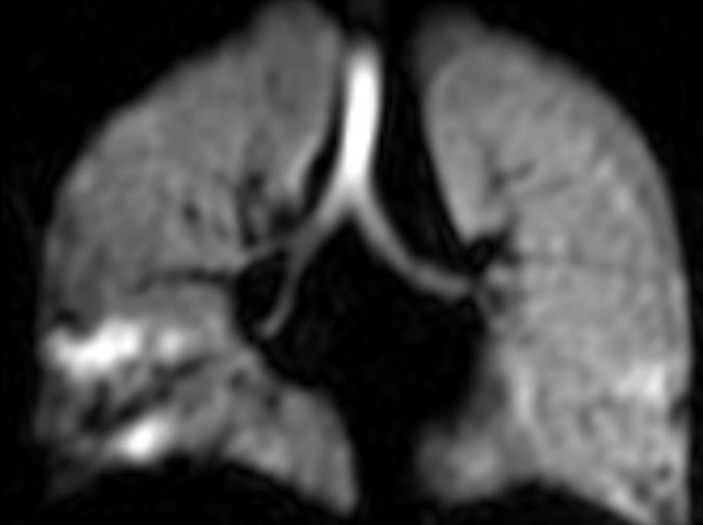
1L natural abundance Xe in 20 min

Low-dose paediatric clinical ^{129}Xe lung imaging

^3He (120 mL)



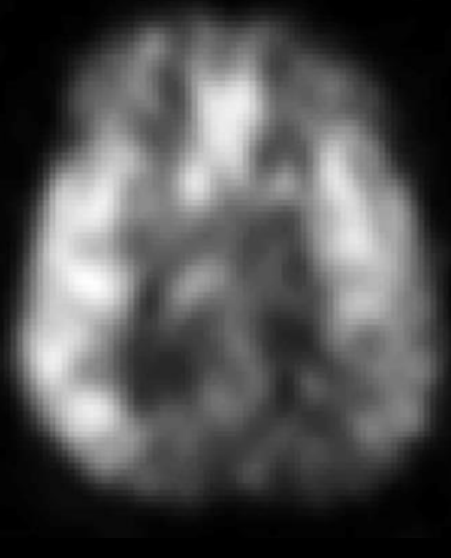
^{129}Xe (250 ml)



250 mL ^{129}Xe dose generated < 5 min

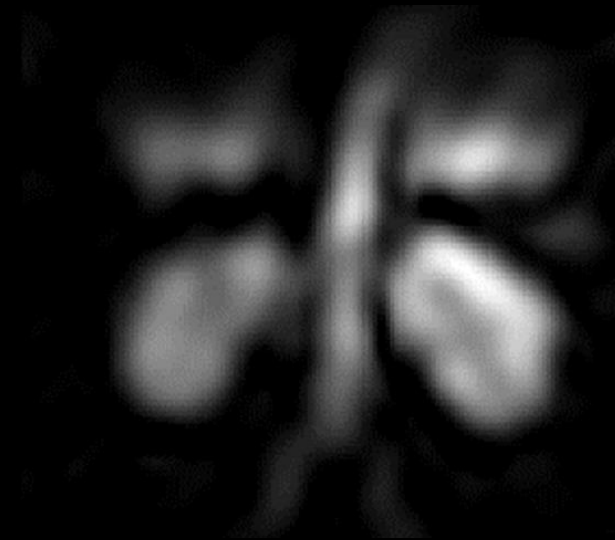
Dissolved ^{129}Xe applications beyond the lungs

1.5 T



^{129}Xe in the brain

3.0 T



^{129}Xe in the kidneys

Bottom
of lungs

Kidneys

Imaging ^{129}Xe straight from the cell

3% xenon on tap, no cryogenic accumulation

Emboli pig no 1



SNR = 34.44, vol = 1L

Emboli pig no 2



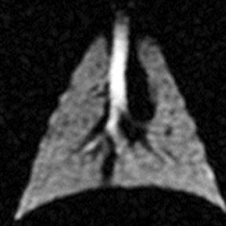
SNR = 41.54, vol = 1L

Healthy pig no 1



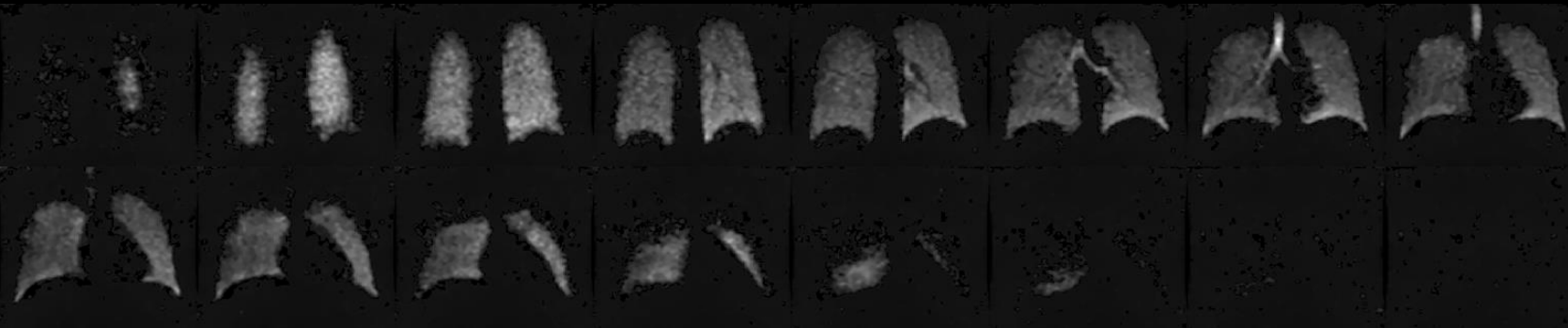
SNR = 28.56, vol = 0.8L

Healthy pig no 2



SNR = 24.46, vol = 0.8L

PORCINE LUNGS



HUMAN LUNGS

Summary

Optimising a polariser system is a complex, multi-parameter problem

[Rb] density critical parameter for process efficiency – generally lower in practice compared with theory

Currently wide range of published exchange rate constants – more work needed

Current unknowns

Cause of SEOP cell deterioration over time

Mechanism driving cell T_1 variations – orientation to B_0 field? Cell T_1 temperature dependence?

Thanks for your attention

Questions?